Tectonics®

RESEARCH ARTICLE
10.1029/2024TC008642

Key Points:

- In situ ^{10}Be basin-wide averaged denudation rates increase eastwards across the strike of the belt with values of up to 1.28 mm/yr
- Denudation rates align with the tectonic structures and are consistent with published incision rates
- The geomorphic and river analysis reflects the coexistence of regional uplift and shallow faulting

Supporting Information:

Supporting Information may be found in the online version of this article.

Correspondence to:

C. Bazzucchi,
chiara.bazzucchi@uniroma3.it

Citation:

Bazzucchi, C., Crosetto, S., Ballato, P., Wittmann, H., Faccenna, C., Scherler, D., et al. (2025). Building topography in a continental subduction orogen: Insights from geomorphic analysis and ^{10}Be denudation rates of the Albanides. *Tectonics*, *44*, e2024TC008642. https://doi.org/10.1029/2024TC008642

Received 3 OCT 2024
Accepted 6 JUL 2025

Author Contributions:

Conceptualization: C. Bazzucchi, S. Crosetto, P. Ballato, C. Faccenna
Formal analysis: C. Bazzucchi
Funding acquisition: C. Faccenna
Investigation: C. Bazzucchi, S. Crosetto
Methodology: H. Wittmann, D. Scherler
Project administration: P. Ballato, C. Faccenna
Supervision: S. Crosetto, P. Ballato, C. Faccenna
Visualization: C. Bazzucchi
Writing – original draft: C. Bazzucchi
Writing – review & editing: C. Bazzucchi, S. Crosetto, P. Ballato, H. Wittmann, C. Faccenna, D. Scherler, F. Rossetti, B. Muceku, C. Durmishi

Building Topography in a Continental Subduction Orogen: Insights From Geomorphic Analysis and ^{10}Be Denudation Rates of the Albanides

C. Bazzucchi[1], S. Crosetto[2], P. Ballato[1], H. Wittmann[2], C. Faccenna[1,2], D. Scherler[2,3], F. Rossetti[1], B. Muceku[4], and C. Durmishi[4]

[1]Department of Science, University of Roma Tre, Rome, Italy, [2]GFZ Helmholtz Centre for Geosciences, Potsdam, Germany, [3]Institute of Geographical Sciences, Free University Berlin, Berlin, Germany, [4]Faculty of Geology and Mining, Polytechnic University of Tirana, Tirana, Albania

Abstract Understanding the relationship between surface and deep geological processes in tectonically active settings is crucial for unraveling the factors controlling landscape evolution and topographic growth. Here, we present the first basin-averaged ^{10}Be-derived denudation rates for the Albanides, a subduction orogen in the Central Mediterranean. By integrating these data with topographic and fluvial analyses, we quantify Quaternary uplift rates and better constrain the spatial and temporal distribution of tectonic deformation, linking the existing long-term thermochronological data with short-term river incision rates. Denudation rates from nine basins range from 0.18 to 1.28 mm/yr, showing a general increase from the external compressional domain to the internal extensional domain. The denudation rates, calculated in catchments assumed to be in dynamic equilibrium and hence interpreted as proxies for uplift, reveal a consistent spatial pattern of tectonic uplift that aligns with active tectonic structures. Higher rates are observed in basins located at the hanging wall of thrust faults or at the footwall of normal faults. The imprint of active tectonics in the landscape is indicated by evidence of river network reorganisation and in the topography. A broad, across-strike increase in mean elevation, combined with local topographic variations along faults, suggests tectonic control on relief, modulated by lithological contrasts. We considered this uplift signal to be potentially controlled by a combination of both deep (e.g., crustal accretion) and shallow (i.e., surface faulting) processes. The former appears to drive the regional topographic pattern, while the latter contributes to localized uplift signals, enhanced denudation rates, and drainage reorganisation.

Plain Language Summary The landscape reflects a complex interplay of lithology, tectonics, erosion, and climate. Deciphering the balance between constructive (tectonics) and destructive (erosion) forces shaping the landscape is a compelling challenge in active mountain ranges like the Albanides. To understand the evolution of the Albanian topography and the drainage systems, we conducted river network analysis and measurements of rare cosmogenic Beryllium isotopes, produced within minerals (in situ ^{10}Be) that serve as natural clocks of erosion rates and are commonly used to assess tectonic uplift. These rates indicate landscape erosion and thus the pace of topographic change. The wide range of rates and their significant spatial variability, along with transient geomorphic features, suggest varying uplift rates across the region. This uplift is likely influenced by two processes operating at different scales: deep processes at a regional scale and surface faulting at a local scale. This research advances our understanding of how tectonic processes shape the landscape in active mountain ranges, providing valuable insights into the geological history in the Albanian orogen up to the present.

1. Introduction

Convergent plate boundaries are among the most dynamic regions on Earth. These margins exhibit the highest topography, resulting from rapid rock uplift that builds mountain ranges (Binnie et al., 2006; Johnson & Harley, 2012; Wobus et al., 2006), driven by shallow and deep-seated processes. Therefore, the topographic evolution reflects the complex interactions among tectonics, climate, and erosion across different spatial and temporal scales. In subduction zones, a constant interplay exists between forces such as slab pull, which lowers topography in forearc and in back-arc regions through extension, and forces that drive surface uplift through crustal accretion and underplating (Crameri et al., 2017; England & Molnar, 1990; Faccenna & Becker, 2020; Schildgen et al., 2014; Whipple, 2009; Whipple & Tucker, 1999; Willet et al., 2001).

The Albanides lie along the eastern margin of the Adria microplate at the transition between continental and oceanic subduction underneath the Dinarides and the Hellenides, respectively (Burchfiel et al., 2008, 2018; Royden & Faccenna, 2018; Royden & Papanikolaou, 2011; van Unen et al., 2019). The relatively high and structured topography (average elevation 700–800 m a.s.l.), along with the coexistence of compressive and extensional tectonic styles over short distances (Burchfiel et al., 2008; D'Agostino et al., 2020, 2022), make this tectonically active region an ideal place to investigate how the deformation is distributed in space and time.

Thermochronological data (Grund, 2023; Muceku et al., 2008; Rossetti et al., 2024) demonstrate that the Albanides have undergone long-term uplift (10^6 yr) since the Middle Miocene. Exhumation estimates range from 1.6 to 3.2 km in north-western Albania (since ∼16 Ma; Grund, 2023) to 3–4 km since Late Miocene-Pliocene in the north-eastern (Muceku et al., 2008) and central-southern Albanides (Rossetti et al., 2024), with a phase of accelerated exhumation occurring between 6 and 4 Ma. On shorter timescales (<200 ka), geomorphological studies on river terraces highlight the combined influence of tectonics and climate. Regional uplift is responsible for the eastward increase in incision rates inferred from river terraces (Carcaillet et al., 2009; Guzmán et al., 2013, 2023), while Quaternary faulting introduces local shifts in the incision rates. Specifically, fluvial incision rates inferred from river terraces range from 0.5 to over 2.0 mm/yr across the Albanides (Guzmán et al., 2023 and references therein), values that appear to be relatively high for a narrow orogen that has only accommodated ∼4 mm/yr of plate convergence during the last 10–5 Ma (Royden & Papanikolaou, 2011). Studies by Carcaillet et al. (2009), Guzmán (2013), and Guzmán et al. (2013, 2023) attribute the spatial and temporal variability in incision rates across central and southern Albania, where they increase from west to east and from longer (>25 ka) to shorter (<25 ka) timescales, to the combined effect of regional uplift and local faulting. To the north, by contrast, the interplay of sea-level changes, glaciation, and active extension is thought to have profoundly influenced drainage evolution (Gemignani et al., 2022).

The existing data set of thermochronological and geomorphological data can be strengthened by basin-averaged denudation rates, which provide a robust framework linking long-term, large-scale evidence of uplift to fluvial incision rates measured over Quaternary timescales. We complement previous river network and morphotectonic analysis of northern Albania (Gemignani et al., 2022) with new data from the central and southern Albanian orogen. These include the first data set of basin-averaged denudation rates in the region, obtained with in situ-produced ^{10}Be in quartz-bearing lithologies. By using the denudation rates as proxy for uplift (a common approach in active tectonic studies; e.g., Binnie et al., 2006; Scherler et al., 2014; Schildgen et al., 2012; Whipple & Tucker, 1999), we analyze their spatial distribution in relation to the main tectonic structures to better constrain the Quaternary tectonic deformation in the Albanides.

2. Geological Background

The Dinarides-Hellenides orogenic system represents a W-verging fold-and-thrust belt resulting from the convergence and collision between the eastern margin of the Adria and the European plates (Figure 1a; Faccenna et al., 2014; Robertson & Shallo, 2000; Royden & Faccenna, 2018; Stampfli & Kozur, 2006; Pearce et al., 2012). Over the Cenozoic, key geodynamic processes took place along this margin, including oceanic and continental subduction, slab rollback and break-off, trench retreat, and continental accretion (Burchfiel et al., 2018; Faccenna et al., 2014; Handy et al., 2015; Jolivet & Brun, 2010; Meço & Aliaj, 2000; Ustaszewski et al., 2008; Zhu et al., 2012). Albania constitutes the northern part of the Northern Hellenides, the central segment of the orogenic system, in literature referred to as Albanides (Argnani, 2013; Frasheri et al., 2009; Lacombe et al., 2009; Muceku et al., 2008; Nieuwland et al., 2001, Figure 1a). The continuity of the belt is supported by paleomagnetic data documenting significant clockwise rotations extending into northern Albania (e.g., Feriozzi et al., 2025; Kissel et al., 1995; Speranza et al., 1992, 1995; Van Hinsbergen et al., 2005).

The paleogeography of the Albanides consists of a Meso-Cenozoic domain of carbonate platforms and deep-water basins, inherited from the Neotethyan system, which have undergone subduction and continental crustal accretion (Figure 1b; Burchfiel et al., 2018; Jolivet et al., 2003; Pearce et al., 2012; Royden, 1993; Royden & Papanikolaou, 2011; Wortel & Spackman, 2000). This orogenic belt is characterized by the coexistence of compression at the frontal zone and extension in the back-arc region (Figure 1c; Kilias et al., 2001; Mazzoli et al., 2008; Muceku et al., 2006; Pearce et al., 2012; Royden & Faccenna, 2018; Tagari et al., 1993), and is structured into several tectono-stratigraphic units that form a large-scale duplex system (Frasheri et al., 2009; Mazzoli et al., 2022; Muceku et al., 2008; Robertson & Shallo, 2000). The internal orogenic sector, at the border

10.1029/2024TC008642

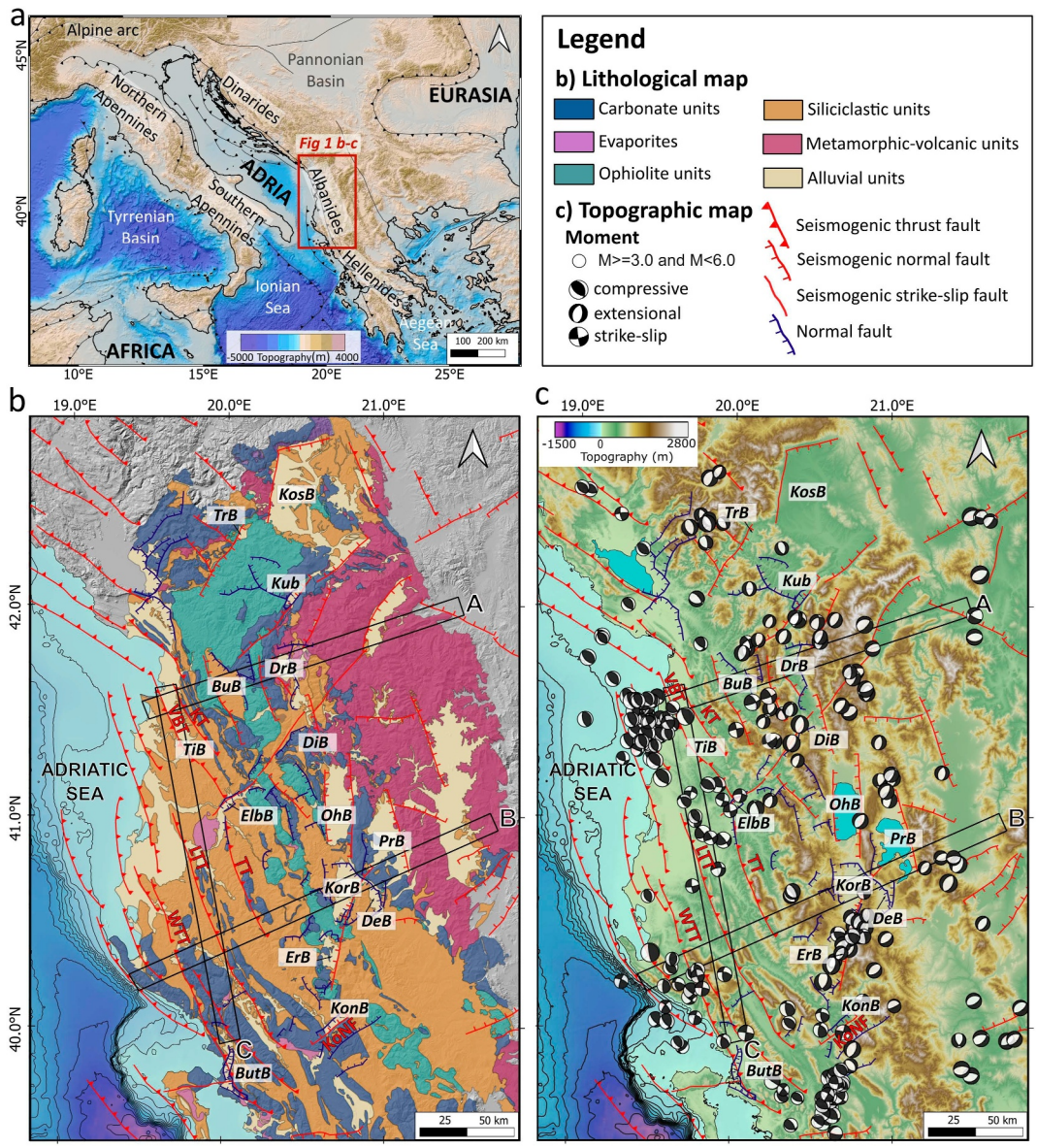

Figure 1. (a) Topographic and tectonic map of the Central Mediterranean region after Faccenna et al. (2014). (b) Lithological map of the study area. Black rectangles indicate the swath profiles shown in Figure 3. (c) Topographic and tectonic map of the study area. Focal mechanisms are sourced from the CMT catalog (Global Centroid Moment Tensor Project, https://www.globalcmt.org/). Seismogenic faults, both compressive and extensional, are shown in red (European Database of Seismogenic Faults, Basili et al., 2013). Normal faults that were active during the Pliocene or Quaternary are depicted in blue (Guzmán et al., 2013; Pashko & Aliaj, 2020). Faults (red labels): KT, Kruja Thrust; VBT, Vorë back-thrust (Vittori et al., 2021); TT, Tomori Thrust; LTT, Lushnje–Tepelenë Thrust; WTT, West Tepelenë Thrust; KoNF, Konitsa Normal Fault. Basins (black labels): TrB, Tropoja; KosB, Kosovo; KuB, Kukesi; BuB, Burrel; DrB, Drin; DiB, Dibër; TiB, Tirana; ElB, Elbasan; OhB, Ohrid; PrB, Prespa; KorB, Korça; DeB, Devolli; ErB, Ersekë; KonB, Konitsa; ButB, Butrinti.

with the Republic of North Macedonia (east of KuB in Figures 1b and 1c), is characterized by a continuous succession of Paleozoic and Mesozoic volcanic, metamorphic, and carbonate deposits (Robertson & Shallo, 2000, Figure 1b). The north-western sector is dominated by carbonate succession (west of TrB in Figures 1b and 1c), while in the central part basalts, serpentines, gabbros, and associated sedimentary deposits constitute the ophiolite complex (Nieuwland et al., 2001; Robertson & Shallo, 2000; Roure et al., 2004), which represent the roof unit of the duplex system. The central part of the Albanides consists of an assemblage of Meso-Cenozoic deep- and shallow-water marine carbonate deposits and ophiolites (Nieuwland et al., 2001; Robertson & Shallo, 2000;

Roure et al., 2004). To the north–east (near to TiB in Figures 1b and 1c), the belt is characterized by foredeep siliciclastic (i.e., flysch like) deposits while, to the south, deep-marine sediments, mainly siliciclastic and carbonate rocks, form westward-verging synclines and anticlines structures (Nieuwland et al., 2001; Robertson & Shallo, 2000; Roure et al., 2013a). In addition, in the central and southern Albanides, Triassic evaporites crop out as diapirs, salt pillows, and salt walls along the base of anticlines or along strike-slip faults, such as the salt pillow cropping out beneath the Tepelenë massif (see Soto et al., 2024). These evaporites represent the basal detachment for the thrust system of the external zone (Mazzoli et al., 2022; Nieuwland et al., 2001; Roure et al., 2004; Soto et al., 2017, 2024), but can be found also in the hinterland within the Drin Basin (DrB in Figures 1b and 1c; Velaj, 2001).

2.1. Tectonic Setting

Currently, instrumental data, including GNSS data (D'Agostino et al., 2020, 2022; Jouanne et al., 2012), modern seismicity (Figure 1c; D'Agostino et al., 2020), and recent larger earthquakes (e.g., Mw 6.9, 1979 Montenegro earthquake and Mw 6.5, 2019 Durres earthquake) demonstrate that the Albanides are a tectonically active mountain range. The spatial pattern of seismicity defines a zonation that includes:

1. An internal area that has been affected by extensional stresses since the Pliocene (Aliaj, 1994, 1998; Burchfiel et al., 2008; Muceku et al., 2008).
2. An external fold- and thrust-belt in the southern sector, deformed by compressional deformation that started before the Pliocene and that, toward the north, becomes a foredeep/wedge top system characterized by post-Pliocene compressional deformation (Argnani, 2013; Frasheri et al., 2009; Lacombe et al., 2009; Muceku et al., 2008; Nieuwland et al., 2001);
3. An offshore undeformed to weakly deformed foreland (Le Goff, 2015; Roure et al., 2004).

In the following sections we provide a description of the internal and external tectonic provinces.

2.1.1. The Internal Extensional Province

The Albanian hinterland constitutes the westernmost part of the South Balkan Extensional System (SBES), a domain with a typical Basin and Range structure (Burchfiel et al., 2008) that developed over the intermediate and internal domains of Albania (Robertson & Shallo, 2000). Two stages of extension can be recognised:

1. Early middle Miocene, involving N–S and NE-SW oriented normal faults accommodating E–W and NW-SE extension due to the retreat of the Northern Hellenic trench (Burchfiel et al., 2008; D'Agostino et al., 2022).
2. Late Miocene, with the development of E–W striking normal faults accommodating N–S oriented extension, likely resulting from the combined effects of the retreat of the Hellenic slab and the westward propagation of the North Anatolian Fault (Burchfiel et al., 2008). In both stages the extensional wave progressively migrated from east to west, reaching each sector of the SBES at different times, leaving behind a series of features such as the typical basin and range landscape (Aliaj et al., 2001).

Thermochronological studies set the onset of extension in the Albanian northeastern hinterland at ∼6 Ma (Burchfiel et al., 2008; D'Agostino et al., 2022; Grund, 2023; Handy et al., 2019; Muceku et al., 2008) with a phase of rapid exhumation (∼1 km/Ma) at 6–4 Ma (Muceku et al., 2008). Other tectono-stratigraphic and geomorphological works allowed to determine the timing of the formation and evolution of the Albanian extensional basins (Aliaj et al., 2001; Burchfiel et al., 2008; D'Agostino et al., 2022; Dufaure et al., 1999; Hoffmann et al., 2010; Lindhorst et al., 2015; Nowack, 1921; Pashko & Aliaj, 2020). Basins related to the E–W extension (Ohrid, Prespa, Dibër, and Devolli) started to form during the late Miocene (Burchfiel et al., 2008; Lindhorst et al., 2015; Pashko & Aliaj, 2020), while others (Korça, Ersekë, Tropoja, Kukës, Drin) started during the early Pliocene (Aliaj et al., 2001; Gemignani et al., 2022; Pashko & Aliaj, 2020) (Figure 1c). The normal faults associated with the extension overprint the previous compressional domain in the Albanian hinterland, as observed in various orogen of the Tethyan realm, where extensional tectonics dissected former contractional structures (e.g., in the Hellenides: Burchfiel et al., 2008; Jolivet et al., 2018; Kilias, 2024; Schenker et al., 2015; in the Apennines: Clementucci et al., 2024; Lanari et al., 2023).

Historical earthquakes, focal mechanisms, and the offset of sedimentary deposits within the basins indicate that most of the border faults were active during the Quaternary (D'Agostino et al., 2022). For instance, the slip rates of the faults related to the south-eastern graben system, which includes the Korça and Ersekë basins, are estimated

to range from 1.3 to >2.0 mm/yr (Guzmán et al., 2013). In addition, the Ohrid, Korça and Drin basins show clear evidence of recent tectonic activity, such as triangular facets, fault scarps, and exposed fault planes (D'Agostino et al., 2020, 2022; Dufaure et al., 1999; Hoffmann et al., 2010; Lindhorst et al., 2015). The basins are now occupied by lakes (Ohrid and Prespa) or alluvial plains (e.g., Korça, Ersekë, Kukës, Devolli, Dibër, Elbasan; Figure 1c). The second wave of extensional tectonics is still migrating westward, having reached, currently, the eastern sector of the Republic of North Macedonia where it is overprinting the former N–S extensional system (Burchfiel et al., 2008).

2.1.2. The External Compressional Province

The external orogenic sector is characterized by a series of fault-related folds that started developing from the early middle Miocene (Aliaj, 1998) and that have accommodated plate convergence over the last 20–15 Ma (Lacombe et al., 2009; Nieuwland et al., 2001; Robertson & Shallo, 2000; Roure et al., 2004). Organized like a typical fold-and-thrust belt landscape, with NW-SE anticlinal ridges related to both thrusting and backthrusting and synclinal valleys, this domain presents a significant along-strike difference in topography and structural configuration (Figure 1c). To the north, anticlinal and synclinal structures extend in a narrow corridor between the Tirana and Burrel Basins, while the entire area from the Tirana Basin to the sea is characterized by a relatively low-relief landscape with a few ridges representing E- to W- verging, fault-related anticlines. Conversely, in the southern sector anticlinal and synclinal structures dominate the landscape extending until the coast (Figure 1c). This external domain experienced the most intense structuring phase before the Pliocene (Bozo et al., 2018) and a new and significant phase of shortening, at least in the central and northern coastal sectors, after the Pliocene (Aliaj, 1998; Bozo et al., 2018).

Evidence of Quaternary uplift is related to the preservation of a regional sequence of 11 river terraces which can be consistently traced and correlated across main valleys of the Vjosa, Osum, Devoll, Erzen, and Mat rivers (Aliaj, 1998; Carcaillet et al., 2009; Guzmán, 2013; Guzmán et al., 2013, 2023; Koci et al., 2018; Nowack, 1921) (Rivers shown in Figure 2). While terrace formation is primarily driven by climatic fluctuations, their long-term preservation cannot be explained by climate alone and instead requires sustained uplift. By comparing terraces formed during the same climatic stage but standing at different elevation, fluvial incision rates of about 0.5–2.8 mm/yr have been estimated over the late Pleistocene (Guzmán et al., 2013, 2023; Mugnier et al., 2024). Additional information comes from the Berati and the Tomori thrust faults displaying vertical slip rates of ∼0.8 and 0.3 mm/yr, respectively, since at least ∼25 ka (Guzmán et al., 2013). Within the fold and thrust belt, however, the Elbasan system is a localized extensional graben basin whose main bounding fault exhibits a slip rate >1 mm/yr for the last ∼25 ka (Guzmán et al., 2013). Ongoing compressional deformation is also testified by seismic events such as the 2019 Durres earthquake (e.g., Teloni et al., 2020; Vittori et al., 2021). Overall, the described pattern of deformation appears to be consistent with GNSS surface velocities that, despite the low spatial resolution, document positive vertical rates of 0.5–1.0 mm/yr in the Northern Hellenides (Serpelloni et al., 2022).

2.2. Morphotectonic Setting

The topography of the Albanides is dominated by a series of NW-SE striking ridges and river valleys delimited to the west by the N–S-trending Albanian coast (Figure 1c). Two regions with different geomorphological characteristics can be distinguished. The central-western Albania region is a low-relief landscape with large alluvial plains and a few NNW-striking ridges. Conversely, to the south, the exposed carbonate rocks form ridges with peaks over 2,000 m separated by valleys and basins primarily composed of more erodible flysch deposits (Figures 1b and 1c). The mean elevation increases in the internal domain, where elevated basins are surrounded by high topography and the landscape is dissected by several normal faults. The transition from the external lowlands to the internal highlands is abrupt in northern and central Albania, while to the south the mountain ridges reach the coast (Koci et al., 2018; Özdemir, 2012).

The Albanian drainage network is characterized by a dense and intricate pattern organized in eight main river systems, namely, from north to south: the Drin, Mat, Erzen, Ishmi, Shkumbin, Devoll-Osum, Vjosa, and Bistrica rivers (Figure 2). These rivers originate in the inland mountainous area and flow toward the Adriatic Sea, crossing a large variety of geological and morphological domains (Guzmán et al., 2013; Özdemir, 2012).

The Drin course is strongly controlled by major tectonic structures in its northward flow (Copley et al., 2009; D'Agostino et al., 2022; Gemignani et al., 2022), before turning abruptly to the west, where it drains basins from

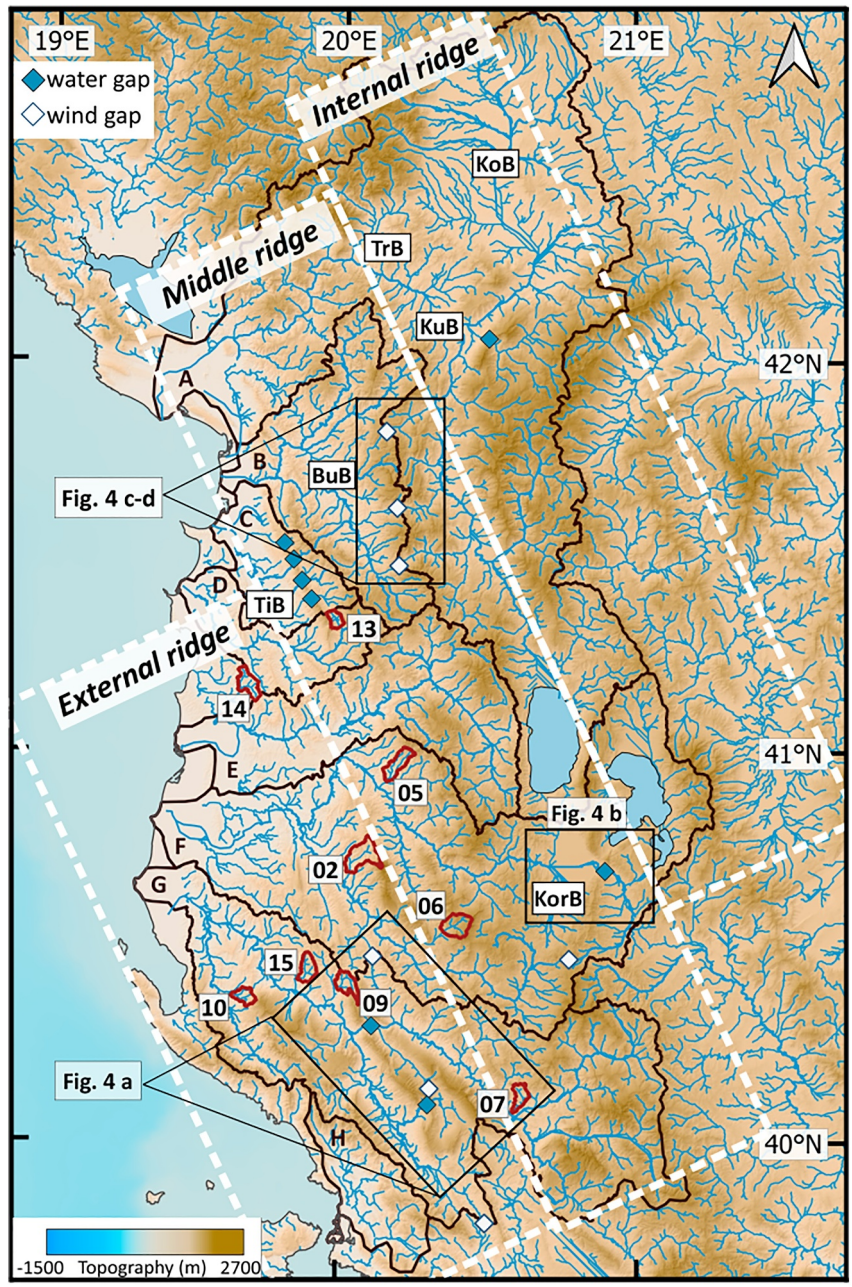

Figure 2. Topographic map depicting the large rivers draining to the Adriatic Sea. Drainage is depicted in light-blue; river drainage basins as thick brown lines; letters at each basin's outlet refer to the river name reported below; numbers correspond to the sampled basins as described in the text and reported in Table S1 of Supporting Information S1. Rivers: A, Drin; B, Mat; C, Ishmi; D, Erzen; E, Shkumbin; F, Devoll-Osum; G, Vjosa; H, Bistrica. Basins' labels as in Figure 1.

north-eastern Albania (east of KuB in Figure 2), the Kosovo basin, and part of the north-western mountainous area (west of TrB in Figure 2). The Mat River drains the Neogene Burrel Basin, while the Ishmi and Erzen rivers drain different sectors of the Tirana basin. The other rivers (Shkumbin, Devoll-Osum, Vjosa, Bistrica) flow from SE to NW draining the internal and the external domains in central Albania.

Differences in relief and lithology between the internal and external domains strongly impact the drainage pattern. The inland mountainous area is mainly composed of resistant rocks such as limestones and ophiolites, which favor the formation of canyons and deep gorges bordered by steep slopes. In particular, the dissolution of limestone combined with water infiltration can cause a lowering of the channel bed and alterations in its

steepness; these changes increase the response time to climate and tectonic forcing, resulting in a steepening of the topography (mostly by the mechanical removal of rocks through rock fall; Ott et al., 2019). This enhanced erosion significantly reduces the possibility of forming and preserving river terraces (Koci et al., 2018), but the abundant bedload resulting from the high slopes generates braided rivers downstream (Balek, 1966; Özdemir, 2012). Conversely, in the westernmost area, highly erodible siliciclastic flysch favors a low-relief landscape and extensive floodplains, allowing rivers to develop a typical meandering morphology.

In central Albania, the Shkumbin and Devoll rivers were originally part of a single river system, the Shkumbin-Paleo-Devoll, with the Paleo-Devoll flowing northward (Guzmán, 2013; Melo, 1961). This is demonstrated by the presence of river terraces along the eastern edge of the plain separating the two rivers, as well as by paleo-current data that confirm the northward flow of the Paleo-Devoll (Guzmán, 2013). Guzmán (2013) proposed that the present-day course of the Devoll River resulted from river capture driven by salt tectonics. Specifically, local subsidence associated with the Dumrë salt diapir (Roure et al., 2004) likely triggered a reorganisation of the drainage system in this region, causing the separation of the two rivers (Guzmán, 2013).

Quaternary fluvial terraces exist along many Albanian rivers, formed in response to climatic changes and preserved due to active tectonics. In particular, their preservation is attributed to a combination of the moderate strength of the bedrock (primarily flysch) and a sustained uplift rate of approximately 1.0 mm/yr in the last 200 ka (Guzmán et al., 2023; Mugnier et al., 2024). Along the major Albanian rivers, 11 generations of terraces, both alluvial and strath, were recognised, mapped, and dated with different techniques (^{14}C, ^{10}Be, U/Th, ESR, TL, ^{36}Cl; Carcaillet et al., 2009; Gemignani et al., 2022; Guzmán, 2013; Guzmán et al., 2013, 2023; Koci et al., 2018; Lewin et al., 1991; Woodward et al., 2001, 2008). These terraces cover an interval of ∼200 ka, and their correlation with the late Pleistocene climatic cycles suggests that climatic variations played a major role in their formation (Guzmán et al., 2013, 2023), consistent with findings from other Mediterranean regions (Macklin et al., 2002). However, significant temporal and spatial variability of the calculated long- (>25 ka) and short-term (<25 ka) incision rates led Guzmán et al. (2013) to suggest the presence of a large-scale tectonic control, as previously suggested by Carcaillet et al. (2009). Specifically, the long-term incision rates of large rivers tend to be consistently lower than short-term incision rates, a pattern that, according to Guzmán et al. (2013), may reflect unsteady uplift, potentially leading to a general increase in incision rates over the past 25 ka. Smaller catchments (Mat and Erzen) yield instead the same incision rates over both short and long timescales (Guzmán et al., 2013). Both Carcaillet et al. (2009) and Guzmán et al. (2013) suggested a dual contribution to the incision rate pattern: regional uplift would ensure the preservation of terraces and control the spatial and temporal variability of incision, while the activity of normal and thrust faults would induce local deviations from the regional trend.

Regional-scale uplift in Albania has been recognised and attributed to deep-seated geodynamic processes (Burchfiel et al., 2008). The long-wavelength uplift pattern correlates with positive residual topography extending from the Albanian interior toward central-eastern Anatolia, suggesting a connection to mantle dynamics (Faccenna & Becker, 2020). Despite evidence of slab break-off in neighboring regions such as the Apennines and the Dinarides (e.g., Handy et al., 2019; Racano et al., 2024), tomographic models indicate that the slab beneath the northern Hellenides, including the Albanides, appears continuous to a depth of 200 km (Kissling, 2024). Furthermore, there is no evidence of mantle-derived volcanism, typically associated with asthenospheric upwelling following slab break-off (Gasperini et al., 2002; Macera et al., 2003a). Volcanic activity, characterized by a calcalkaline signature typical of subduction-related processes (e.g., Ernst, 2010), only begins to emerge further inland in Macedonia (Božović et al., 2013; Brombin et al., 2022). An alternative mechanism proposed for uplift and crustal thickening in the Albanides is crustal underplating (Burchfiel et al., 2018). Such mechanism, which has been active at least since ∼35 Ma (Burchfiel et al., 2018), is thought to be responsible of the significant crustal thickness of the Albanides (∼50 km, Burchfiel et al., 2018) and to have triggered the activation of deep compressive structures that generated periods of rapid uplift associated with long-wavelength (10^6 yrs) topographic development (see Rossetti et al., 2024, their Figure 5).

2.3. Climate and Paleoclimate

Present-day climatic conditions are homogeneous over the entire Albanian region (Mugnier et al., 2024), with a Mediterranean climate characterized by mild, rainy winters and hot, dry summers (Guzmán et al., 2023). Paleoclimate reconstructions from the well-preserved sediments of Lake Ohrid (Francke et al., 2016; Sadori

et al., 2016) and Lake Ioannina in Greece (Roucoux et al., 2008) provide insights into climate variability over the past 500 ka, while the record of preserved river terraces in Albania documents climate changes over the last 200 ka (Carcaillet et al., 2009; Gemignani et al., 2022; Guzmán et al., 2013, 2023; Koci et al., 2018; Lewin et al., 1991; Woodward et al., 2001, 2008). These records highlight the strong influence in terraces formation of the Quaternary climate fluctuations, where cold, dry glacial periods alternate to warm, humid interglacials. Recent studies (Guzmán et al., 2023; Mugnier et al., 2024) suggest that the abandonment of terrace surfaces was primarily driven by climatic variations and generally occurred synchronously with the transitions from cold to warm periods. During these transitional phases, the sudden increase in precipitation favors the increase in sediment supply from previously glaciated or unvegetated areas, thereby affecting the geomorphic response of the fluvial system to these rapid variations. Accordingly, the authors propose that catchments with extensive high-altitude areas, more prone to glaciation and sparse vegetation, tend to develop fill terraces, whereas those distributed in low-altitude areas, less or not at all affected by glaciation and vegetation scarcity, predominantly form strath terraces at these transition events (Guzmán et al., 2023; Mugnier et al., 2024).

Glaciation also played a role in the drainage evolution in specific regions of Albania (Hughes, 2007; Hughes et al., 2006; Hughes & Woodward, 2017; Leontaritis et al., 2020; Woodward et al., 2008). The glacial imprints have been investigated in detail in some areas, particularly in northwest Albanides (Gemignani et al., 2022; Hughes, 2009), , where glacial melting combined with sea-level and climate fluctuations contributed to terrace formation in the Tropoja Basin along the Drin River system, triggering episodes of paleolake overspilling, river capture, and drainage integration (Gemignani et al., 2022). In the southern Albanides, glaciers influenced the erosional and depositional cycles of the upper and middle parts of the Vjosa River (east of Gjirokastër valley: Louis, 1926; Leontaritis et al., 2020; the Voidomatis Valley; Mugnier et al., 2024; Woodward et al., 2008). Evidence of glaciation was found also in central Albania, particularly in the region of Lake Ohrid and Prespa (western Republic of North Macedonia), with glaciers active during the Last Glacial Maximum (Gromig et al., 2018; Ribolini et al., 2011, 2018). However, due to their limited size and the karstic bedrock, lacustrine sediments do not indicate the presence of proximal glaciers, suggesting a restricted extent of these ice bodies (Gromig et al., 2018; Ribolini et al., 2011). Similarly, no evidence of paleo-glaciers was identified within the Osum and Devoll river catchments (Mugnier et al., 2024).

3. Methodology

To study landscape evolution within the Albanides and decipher the relative significance of the climatic and tectonic factors influencing it, we combine detailed topographic analyses with the quantification of basin-wide denudation rates using in situ-produced ^{10}Be in quartz-bearing lithologies (Granger et al., 1996; Lal, 1991; von Blanckenburg, 2005). Following the topographic and tectonic organisation of the belt, we divided the study area in three NW-SE-oriented, orogen-parallel sub-areas defined as external (compressive), middle and internal (extensive) ridges (Figure 2). We will refer to this nomenclature throughout the text.

3.1. Topographic Analysis

The topographic analysis aimed at identifying the main factors controlling the Albanian landscape. Typically, lithology has a strong influence on topography: lithotypes with higher resistance to mechanical erosion form steep slopes, while highly erodible lithotypes are associated with shallow slopes and gentler morphology. Therefore, the geological map of Albania (1:200.000; Albanian Geological Survey, 2002) was used in combination with a 30-m resolution Digital Elevation Model (DEM) and satellite imagery to conduct the topographic analysis. The DEM was processed in MATLAB using the software packages TopoToolbox (Schwanghart & Scherler, 2014) and Topographic Analysis Kit (Forte & Whipple, 2019). In the topographic analysis, high elevation, steep slope angles, and local relief are commonly used as indicators of tectonic deformation, whether recent or inherited from older geological events. For this reason, we employed swath profiles with widths of 10, 5, and 1 km to detect topographic evidence of deformation with respect to tectonic structures and lithology. We ground-truthed the remote analysis during three field campaigns, when we also validated the fault kinematics reported in literature, and made additional observations on the drainage network.

A 400-m resolution DEM was used to obtain filtered DEM with different spatial windows (wavelength of 12, 25, 50, 75, 100 km) aimed at highlighting larger-scale topographic signals potentially associated with deeper contributions. The denudation rates from the sampled basins were compared with topographic metrics obtained from

the 30 m DEM (Schwanghart & Scherler, 2014). The average elevation of the basin was computed using the mean function applied to the vertical component of DEM. Hillslope was calculated with the gradient 8 function, which provides the steepest downward gradient of the DEM using 8-connected neighboring pixels. Local relief was performed within a circular window of 1 km radius due to the average size of the basins, whose areas typically span from 20 to 60 km^2 and that are often located near topographically elevated regions composed of carbonates, which may impact the analysis. The mean annual precipitation (in mm/yr) was calculated for each basin using the WorldClim grid database (Fick & Hijmans, 2017), with a spatial resolution of 2.5 min (~21 km^2 at the equator), for each month of the year over a period of 11 years (2011–2021).

3.2. River Network Analysis

The river network analysis is based on the capability of rivers to effectively respond to perturbations within the system, whether caused by climatic variations or tectonic activity, which affect the relative base level (see Supporting Information S1 for details) (Hack, 1957b; Kirby & Whipple, 2001; Whittaker, 2012; Wobus et al., 2010).

Using the TopoToolbox (Schwanghart & Scherler, 2014), we extracted the drainage network to examine the organisation of the drainage in relation to lithology, referring to the geological map of Albania (Albanian Geological Survey, 2002), and major tectonic structures (Database EDSF, Guzmán et al., 2013; Pashko & Aliaj, 2020; Basili et al., 2013). The main rivers of Albania were identified based on a minimum upstream area of 500 km^2. In contrast, the analysis of the total drainage network was conducted using a threshold area for channel head initiation of 1 km^2. The mean normalized steepness index (k_{sn}) (Kirby & Whipple, 2012; Wobus et al., 2006) along the stream network was computed with a reference concavity of 0.45 and used for comparison with denudation rates.

3.3. Cosmogenic ^{10}Be Denudation Rates

We selected 9 basins from the central and southern parts of the study area (Figure 2), where quartz-bearing units prevail. The analyzed basins drain siliciclastic flysch units, however, in three basins, small sectors of carbonate or ophiolite were present. These were excluded from the analysis to ensure consistent lithological conditions when calculating topographic metrics and production rates. The selected basins have drainage areas between 21 and 60 km^2, sufficiently large to avoid potential issues from shallow landslides (Niemi et al., 2005), but small enough to have relatively uniform topographic and geologic characteristics (Ouimet et al., 2009). Well-graded longitudinal river profiles suggest equilibrium conditions where erosion and uplift are balanced (Howard & Kerby, 1983; Whipple & Tucker, 1999, see Supporting Information S1). The catchments are, as far as possible, located in regions minimally impacted by anthropogenic activity, with sampling sites positioned >200 m upstream from confluences with trunk rivers to ensure well-defined source areas, and, when possible, away from disturbances such as landslides, construction sites, and villages. At each site, we collected approximately 5 kg of quartz-bearing sediment from the active channel.

All samples were processed in the Helmholtz Laboratory for the Geochemistry of the Earth Surface (HELGES) at the GFZ Helmholtz Center for Geosciences, in Potsdam (Germany) following the methodology of von Blanckenburg et al. (2004). Samples were dried and sieved (dry and wet sieving) to obtain the 125 μm – 1 mm fraction for quartz purification. To remove the abundant carbonates, the samples were first leached with concentrated HCl (>37%) and subsequently with weak HCl (9%). The next steps involved froth flotation with dodecylamine to physically remove feldspars and micas, and a treatment with ortho-phosphoric acid at elevated temperature (220–250°C) and several leachings with weak HF (5%, 2%, 1%) to dissolve the remaining feldspars and micas.

For the chemical separation of Beryllium, 30–40 g of pure quartz underwent final leaching with concentrated HF (>48%), followed by spiking with ~0.15 mg of ^{9}Be carrier, ion exchange chromatography, precipitation in an alkaline solution of ammonia, and oxidation at 1,000°C. The BeO was pressed into cathodes for accelerator mass spectrometry (AMS) measurement of $^{10}Be/^9Be$ ratios at the Cologne AMS of the University of Cologne (Dewald et al., 2013), which were normalized to standards KN1-6-2 and KN1-5-3 (having nominal $^{10}Be/^9Be$ ratios of 5.35×10^{-13} and 6.32×10^{-12}, respectively, which are consistent with the 07KNSTD standard and with a ^{10}Be half-life of $1.36 \pm 0.07 \times 10^6$ yr, Nishiizumi et al., 2007).

To calculate denudation rates, we used the Matlab functions of the CRONUS online calculator v. 2.3 (Balco et al., 2008), in conjunction with the functions of the TopoToolbox (Schwanghart & Scherler, 2014) and the 30-m resolution DEM. Measured $^{10}Be/^{9}Be$ ratios ranged between 1.61×10^{-14} and 6.56×10^{-14}. For the calculation of ^{10}Be we applied a $^{10}Be/^{9}Be$ blank correction using the blanks processed alongside the two batches of samples. The blank correction values were 1.37×10^{-14} ($n = 1$ blank) for sample #02 (first batch), and 3.59×10^{-15} ($n = 1$ blank) for the rest of the samples (second batch). We assumed a density of the bedrock in the catchment of 2.7 g/cm^3. Production rates were calculated for each basin using the time-dependent Lal/Stone scaling scheme (Lm) (Balco et al., 2008) calibrated to a reference production rate at sea-level and high latitude (SLHL) of 4.00 ± 0.32 (Borchers et al., 2016; Phillips et al., 2016). In three (#05, #09, #13) of the catchments, exposures of carbonates and ophiolites, as indicated in the lithological map (Figure 1b), were excluded in calculation of production rates. The details of the calculation are reported in the SI and in the Zenodo repository at the following link: https://doi.org/10.5281/zenodo.15244016.

3.4. Calculation of Erosion Rates From Thermochronological Data

To derive erosion rates from cooling ages, we applied the analytical method implemented in Agetoedot (Willett & Brandon, 2013). This method inverts individual cooling ages to erosion rates by solving for closure temperatures based on the Dodson (1973) equation and accounts for the effects of heat advection caused by erosion. The approach assumes a constant cooling rate during erosion, such that the observed cooling ages represent the time elapsed since samples passed through their respective closure temperatures (Dodson, 1973).

The erosion rates are assumed to remain constant from the onset of erosion, while the geothermal gradient increases with ongoing erosion. The kinetic parameters for helium diffusion in apatite were adopted from Gautheron et al. (2009). The closure depth is determined as the intersection of the geotherm with the corresponding closure temperature.

The method assumes steady-state topography, with the thermal influence of topography being wavelength-dependent (Braun, 2003). This influence is approximated by calculating a mean elevation. To account for this effect, an averaging circle with a radius of 5 km for the AHe (Willett & Brandon, 2013) data was used to compute the mean elevation. To calculate erosion rates from cooling ages, we used estimates of the modern geothermal gradient, the onset time of erosion, and the surface temperature as input parameters (see, Table S3 in Supporting Information S1). The onset time of erosion was set to the oldest AFT age reported in Rossetti et al. (2024), while the surface temperature was assumed to be 15°C. Geothermal gradient bounds of 20°C/km (Cermak et al., 1996) and 30°C/km were chosen to test the sensitivity of erosion rates. The resulting ranges of erosion rates are reported in the Table S3 of Supporting Information S1 and provide a comprehensive representation of the variability associated with the different geothermal gradients. Additionally, an average erosion rate was calculated by taking the mean of the rates derived using gradients of 20 30°C/km.

4. Results

4.1. Regional Topographic Analysis

Lithology appears to be a key factor controlling the Albanian topography: limestones, ophiolites, and specific members of the metamorphic/volcanic complex are associated with steep slopes, while gentler slopes indicate the presence of siliciclastic flysch and Quaternary basin-filling deposits. However, the three swath profiles of Figure 3 reveal a variation in elevation both along and across the strike of the belt.

Perpendicular to the strike there is a significant, long-wavelength increase of topography as the tectonic regime shifts from compression to extension (Figures 3a and 3b): to the west, thrust faults are responsible for the formation of ridges, while to the east normal faults create large basins bordered by steep slopes, with a few mountain peaks over 2,000 m. In particular, the swath profile of Figure 3b shows a large-scale W–E increase in the mean elevation, while the topographic relief remains relatively constant. At the local scale, sharp differences in topography often reflect the presence of faults, which increase the elevation of the hanging wall and footwall of thrust and normal faults, respectively. Particularly sharp and elevated ridges are observed in the western part of the southern swath (Figure 3b), where the effect of thrusting is amplified by the presence of carbonates in proximity of the shoreline.

10.1029/2024TC008642

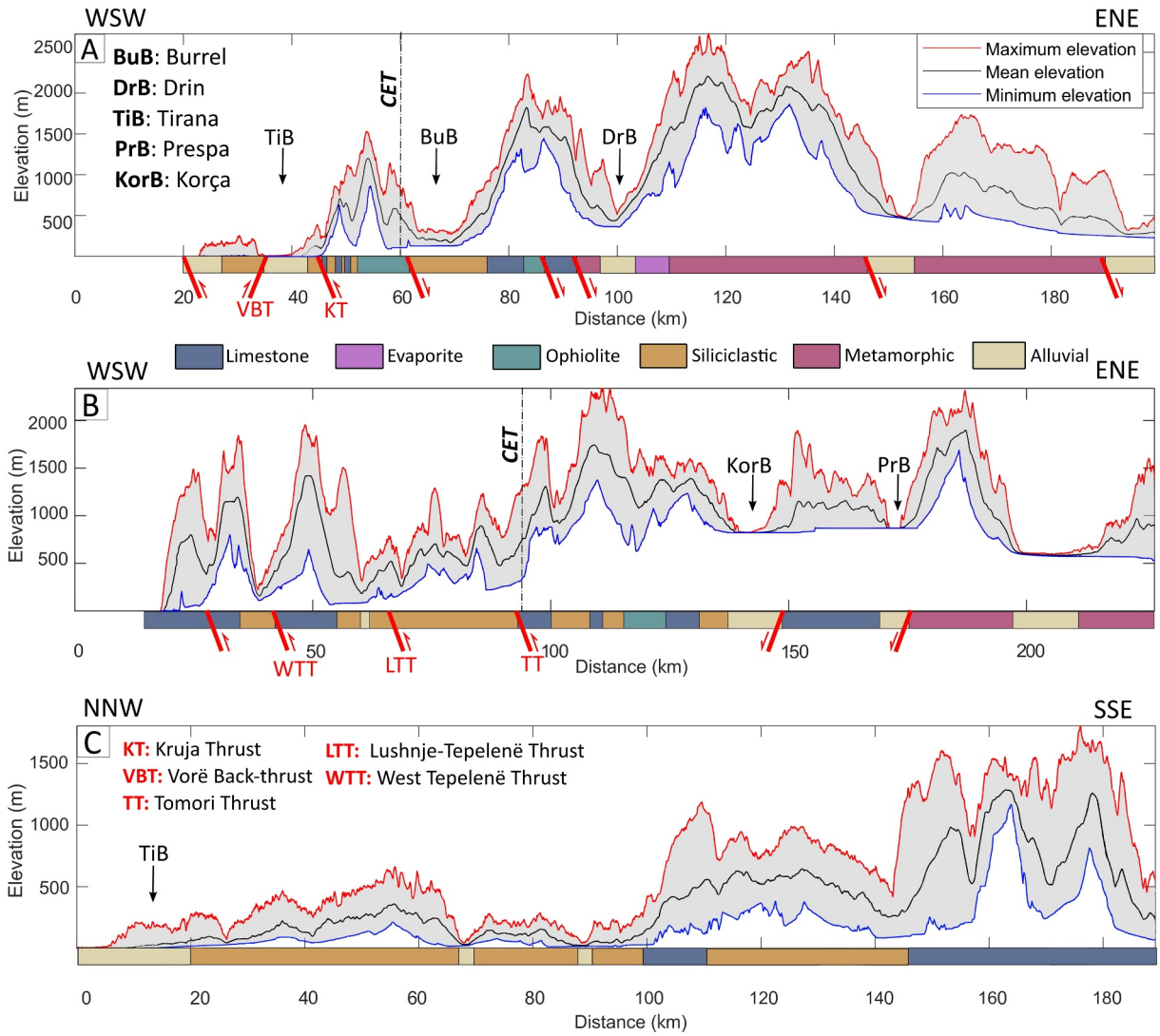

Figure 3. Topographic swath profiles: a and b are perpendicular, and c is parallel to the strike of the belt (swath traces in Figures 1b and 1c). Below each profile, the lithology of the geological units and the tectonic structures crossed by the profile trace are indicated. The point where the fault trace crosses the center of the swath in the map (cfr. Figure 1c) determines the location of the fault (red lines) along the profiles. CET notation indicates the "compression-extension transition." Basin labels are reported in a, fault labels are in c.

The orogen-parallel swath profile (Figure 3c) lies entirely within the compressional domain. Here, the topography is characterized by a sharp change in elevation from a relatively low relief landscape, with mean elevations of 200–300 m in the northern part, to mean heights above 500 m in the south, with mountain peaks in the region reaching elevations of more than 2,000 m. In the northern part, surface evidence of faulting is minimal, and thrusts only create low-elevation ridges with shallow slopes.

4.2. River Analysis

Evidence of drainage reorganisation is observed in different parts of the belt. The overall topographic configuration and NW-SE-elongated ridges characterizing the Albanian landscape force the E–W-flowing rivers to adapt their course to the topography: streams generally flow mostly parallel to the ridges, and locally incise them perpendicularly to their strike to reach the sea. This process creates water gaps through the ridges, as observed for example, along the Vjosa river, north of the Gjirokastër valley system, and along the Devoll river, within the Korça basin (Figures 4a and 4b, respectively), and wind gaps, such as along the ridge separating the Burrel and the Drin basins (Figure 4c).

10.1029/2024TC008642

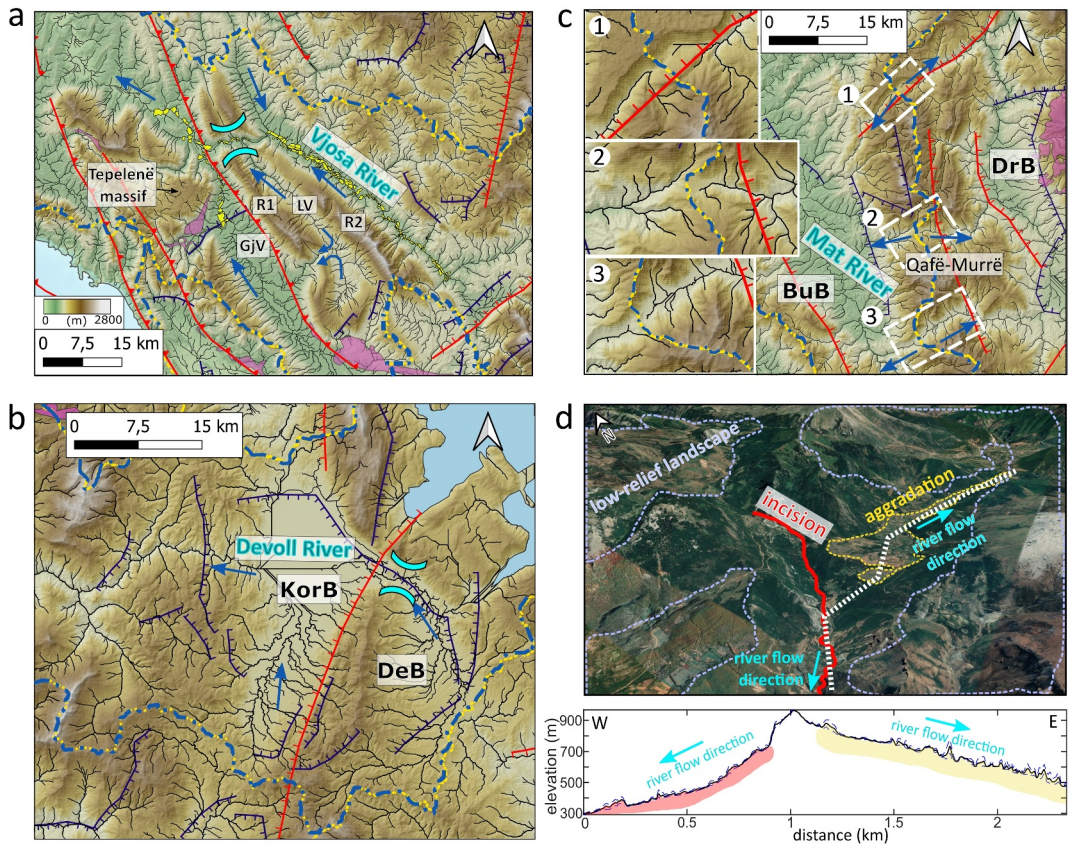

Figure 4. Evidence of drainage reorganisation on the DEMs of the (a) Gjirokastër valley system, (b) Korça and Devolli basins, (c) Burrel and Drin basins (locations in Figure 2), depicting: the drainage system in black, main drainage divide in blue-and-yellow dash-dot line, active faults in red, inactive faults in dark blue. Pink polygons in (a) represent mapped salt diapirs. Blue arrows indicate the current river flow direction; opposite brackets symbol ")(" in light-blue indicates the location of water gaps; yellow polygons in (a) represent major river terraces. Rectangles in (c) indicate the location of the insets. GjV, Gjirokastër valley; R1 and R2, ridge1 and ridge2; LV, longitudinal valley. DrB, Drin basin; BuB, Burrel basin; KorB, Korça basin; DeB, Devolli basin. (d) Top: Google Earth view of the Qafë Murrë valley (corresponding to inset 2 in (c)); the dashed white line is the trace of the swath profile at the bottom. Map's locations are shown in Figure 2.

Figure 4a depicts the Vjosa drainage system in the area of the water gap: the westward-flowing Vjosa river cuts perpendicularly two NW-SE-elongated ridges (R1, R2) that are separated by an elevated longitudinal valley (LV) whose bottom lies at elevations of up to 800 m. The longitudinal valley presents two drainage basins: one flowing toward the NW and directly into the Vjosa, one draining toward the SE and then sharply turning SW into the Gjirokastër valley (GjV in Figure 3a). The SE-draining river is mostly in aggradation, and incision is confined downstream as the stream cuts through R1 and flows into the Gjirokastër valley, where aggradation occurs. Conversely, in the lower Gjirokastër valley and NE of the Tepelenë massif, bounded to the SE by a large salt diapir, alluvial deposits are incised and form terraces (yellow polygons in Figure 4a and depicted in Figure 5a).

In Figure 4b, the Korça and Devolli basins system, located in the southern part of the middle ridge, is reported. The two alluvial plains are separated by a NNE-trending ridge extending along the footwall of the active normal fault bounding the eastern margin of the Korça basin. The two basins are connected by a water gap along the Devoll River, which originates in the Devolli basin, flows northward, then turns to the west cutting through the ridge in a narrow corridor to reach the Korça basin.

Figure 4c shows the location of the wind gaps along the drainage divide between streams flowing into the Burrel and the Drin basins. The valleys of the eastward-flowing streams widen upstream, opposite to the typical downstream widening, and show evidence of fluvial aggradation at the drainage divide (Figure 4d, top), possibly indicative of a previous westward flow. Tributary streams joining the main river at right or obtuse angles with respect to the main trunk (independently from lithology; see insets in Figure 4c) indicate stream flow reversal

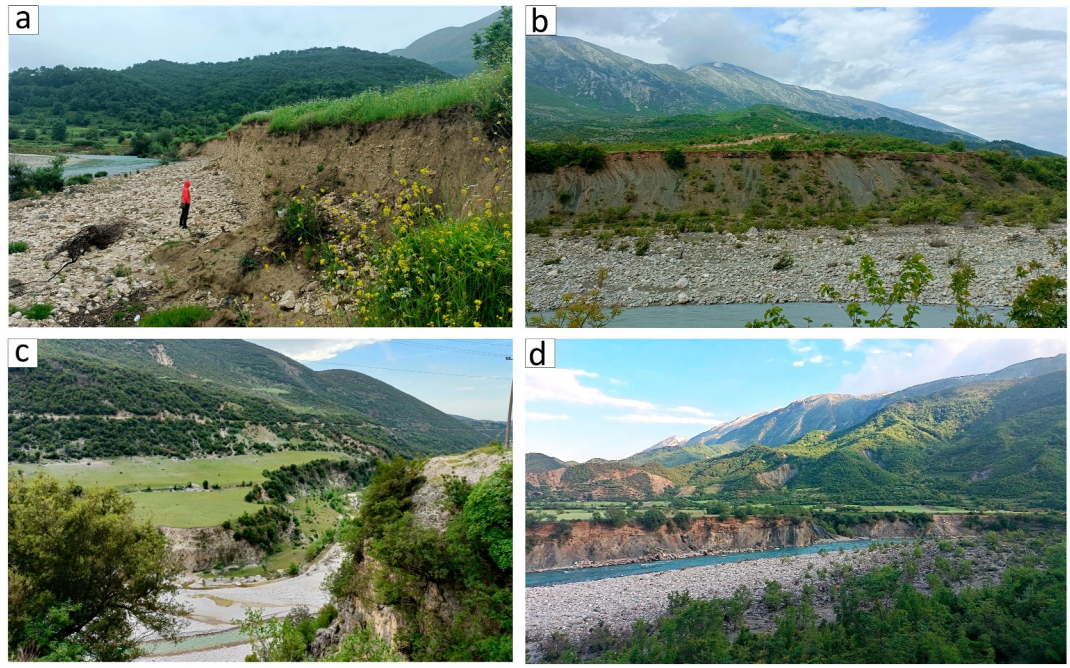

Figure 5. Field photos depicting alluvial and strath river terraces. (a) Incised terraces in the lower valley of Gjirokastër; (b, c, d) strath terraces with minimal sediment cover resting directly on flysch bedrock along the valley west of R2 (b, d), and on limestone bedrock near Tepelenë (c).

(Twidale, 2004). Stream flow reversal is also supported by the longitudinal topographic swath profile along the Qafë-Murrë valley (Figure 4d, bottom), which reveals a gently dipping eastern flank, characterized by aggradation, and a steeper western flank, showing intense incision.

River terraces indicative of active incision can be observed over the entire Albanian region (Figure 5). These include alluvial terraces, resulting from an aggradation phase followed by sediment incision (Figure 5a); as well strath terraces, where a high magnitude of incision causes the erosion of the sediment cover and of the underlying bedrock (Figures 5b–5d).

4.3. ^{10}Be Basin-Averaged Denudation Rates and Basin Characteristics

^{10}Be-derived basin-averaged denudation rates show significant variability across the study area, ranging between 0.18 and 1.28 mm/yr (Figure 6). We categorized our samples into two groups based on their location along the middle (red) or the external (yellow) ridge and are presented in their tectonic context (see, Figure S1 in Supporting Information S1).

The basins along the middle ridge (#05, #06, #07, #13) yield relatively high denudation rates (0.48–1.28 mm/yr; Figure 6), Starting from the north (Figure 6), basin #13 is situated in the hanging wall of the active Kruja thrust (KT) and also within the hanging wall of the normal fault bordering the Burrel basin (Vittori et al., 2021). Sample #5 is not directly located in the vicinity of any faults but lies within a region highly affected by normal faulting of the Elbasan normal fault system and by the Tomori thrust. This thrust likely impacts also sample #6, which exhibits the highest denudation rate in the region. However, the high values of sample #6 may be influenced by its location, a high relief mountainous area characterized by marl-rich flysch, which is highly susceptible to erosion and landsliding (see, Figure S2 in Supporting Information S1). Sample #7 is located in the middle of the Ersëke and Konitsa normal fault systems.

Conversely, samples along the external ridge show slightly lower denudation rates (0.18–0.82 mm/yr; Figure 6). Despite the scattered distribution of the data, it is possible to identify two clusters: a fast-eroding cluster (#02, #09 and #14, 0.39, 0.82 and 0.70 mm/yr, respectively) and a slowly eroding cluster (#10 and #15, 0.25 and 0.18 mm/yr, respectively). However, these two clusters do not reflect a consistent spatial pattern (Figure 6). In fact, in the south the basins #10 and #15 show comparable low denudation rates, compared to sample #09 that,

10.1029/2024TC008642

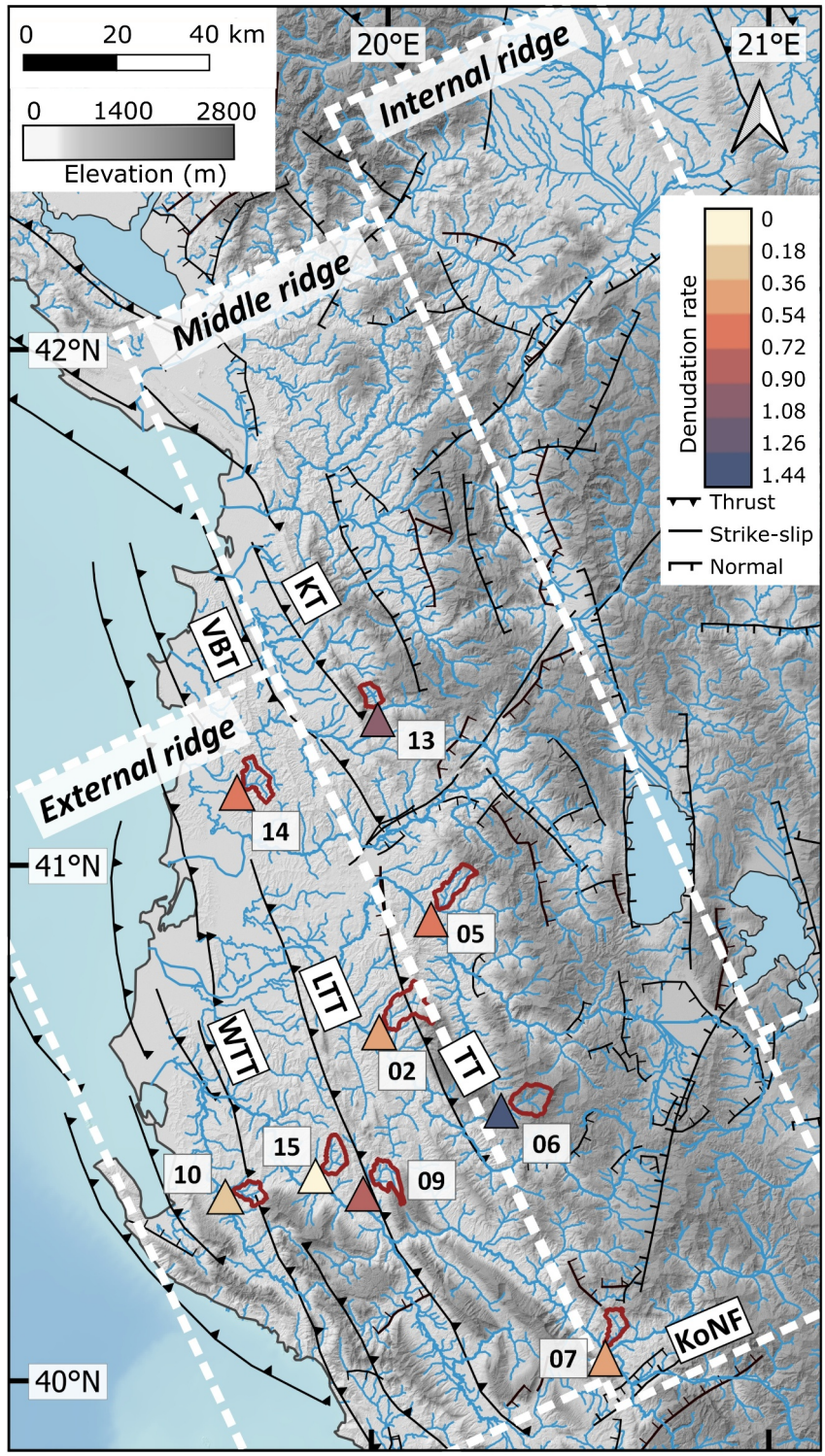

Figure 6. Topographic map displaying the drainage system (light-blue color), the main faults in black, and the sampled basins as triangles color-coded by denudation rate value, distributed along the external and middle ridges.

despite its proximity to the other two, shows a high denudation rate. Samples #10 and #15 lie on the footwall of thrust faults (WTT and LTT, respectively), while sample #09 is located on the hanging wall of LTT. The denudation rates increase toward the north along the strike of the belt (#02 and #14). Sample #2 (0.39 mm/yr),

located at the boundary between the external and middle ridges, partially lies on the hanging wall of the Tomori Thrust (TT). Sample #14 is located in the south-western part of the Tirana Basin, characterized by several active thrust faults (Mazzoli et al., 2022; Vittori et al., 2021). Specifically, this basin lies on the western side of the ridge generated by the activity of the Vorë back thrust (VBT), and this area lies also above the deep thrust ramp responsible for the 2019 Durres seismic sequence (Teloni et al., 2020; Vittori et al., 2021). Overall, higher denudation rates characterize the middle ridge with an average of 0.85 ± 0.12 mm/yr ($n = 4$), while the external ridge presents predominantly lower denudation rates with an average of 0.47 ± 0.06 mm/yr ($n = 5$). The exceptions are represented by sample #09 (0.82 mm/yr) in the southern external ridge, and sample #14 (0.70 mm/yr) in the northern external ridge area, respectively.

We compared the denudation rate values to four topographic metrics: mean basin elevation, mean basin slope, mean basin normalized channel steepness (k_{sn}), and mean basin 1-km local relief (see Supporting Information S1). For each comparison the respective R^2 was calculated. Although these metrics represent potential controlling factors on denudation rate, they do not vary substantially across the study area with respect to denudation rates. A positive correlation is only observed between denudation rates and slope values ($R^2 = 0.78$) (see, Figure S1c in Supporting Information S1), with higher denudation rates corresponding to steeper slopes. However, denudation rates show significant variability within a narrower range of slope angles (15°–20°).

4.4. Erosion Rates From Thermochronology

The erosion rates derived from cooling ages presented in Rossetti et al. (2024) range between 0.2 and 0.8 mm/yr (see, Table S3 in Supporting Information S1). The samples are distributed along a SSW–NNE-oriented transect, intersecting the external and middle ridges according to our subdivision of the study area. Samples from 4 to 8 in Rossetti et al. (2024, Figures 2a and 2b) are located in the southern sector of the external ridge. The highest erosion rates are associated with the youngest AHe ages (Samples 5 and 6, Figures 2a and 2b in Rossetti et al., 2024; 3.1–3.9 Ma, respectively) and are situated in the Gjirokastër area, in the more internal part of the external ridge. Samples 9 to 12 are located in proximity of the middle ridge. Samples 9 and 10 are positioned at the transition between the external and the middle ridges, while samples 11 and 12 are located farther inland, west of the Korça Basin. Here, the lowest erosion rate corresponds to the oldest AHe age (Sample 10, Figures 2a and 2b in Rossetti et al., 2024; 7.2 Ma) located in the proximity of the Tomori Thrust (TT in Figure 1).

For a modern geothermal gradient of 20°C/km, the rates range from 0.3 to 0.8 mm/yr, whereas for a geothermal gradient of 30°C/km, they range from 0.2 to 0.6; mm/yr (See, Table S3 in Supporting Information S1). Despite the significant influence of the assumed geothermal gradient on the estimated erosion rates, the overall pattern in southern Albania consistently shows increasing average erosion rates from the outermost sectors of the external ridge toward the hinterland.

5. Discussion

5.1. Morphotectonics and River Network

5.1.1. Topographic Architecture and Tectonic Controls

The topographic configuration of the Albanides is characterized by high-elevation mountainous areas, pronounced topographic relief, narrow river valleys, and high-standing alluvial basins (e.g., Korça basin). The most rugged and mountainous regions of Albania are in the interior of the orogen, where the mean topography is significantly higher than the coastal areas and increases eastwards across the strike of the belt. This is especially evident along the middle and internal ridges, which feature high-relief terrain and deeply incised valleys (Figure 2). On a local scale, the topography is clearly influenced by the combination of compressive and extensional tectonics, with ridges corresponding to the hanging wall and footwall of thrust and normal faults, respectively, and valleys in the faults' footwall and hanging wall. Lithology further amplifies the tectonic effects due to different rock erodibility: resistant lithologies form steep slopes, while highly erodible lithotypes result in a gentle morphology.

Despite the local impact of surface faulting, the swath profiles in Figures 3a and 3b show that the mean elevation increases from west to east in the shape of a bulge, while topographic relief remains constant. A similar increase across strike is observed in the regional incision rates inferred from river terraces along rivers in central and southern Albania (Carcaillet et al., 2009; Guzmán et al., 2013, 2023). The bulging shape of this topographic signal

suggests, in addition to surface faulting and lithological control, the presence of deep mechanisms that could sustain the regional high relief. This may also partially explain the sharp along-strike variation of elevation, highlighted in the swath profile of Figure 3c.

5.1.2. Tectonics and River Network

The morphotectonic and river analysis revealed a continuous interaction between river network and local tectonics. To the south, a sequence of elevated and steep ridges (anticlines) and narrow valleys (synclines) reflects the activity of the thrusts bringing to the surface lithotypes with significant difference in erodibility, namely carbonates and siliciclastic flysch. The presence of water gaps within anticlinal structures implies that rivers predate the formation of the anticlines, indicating that their erosive power was sufficient to persist in eroding and flowing across the growing anticline during tectonic deformation, a characteristic also observed in other fold-and-thrust belts, such as the Zagros Mountains (Ramsey et al., 2008) and the Jura Mountains (Yanites et al., 2017). This phenomenon is particularly pronounced in carbonate ridges, where both physical erosion and chemical dissolution contribute to vertical incision (Ott et al., 2019), resulting in the formation of narrow valleys with steep walls. The best example of river-growing anticline interaction is represented by the Vjosa river, forming a narrow water gap through one of the ridges close to Gjirokastër (see Figure 4a).

Tectonics may also explain the evolution of the Gjirokaster valley. The presence of basin infill/alluvial deposits over the entire valley, with incision limited to the lower part of the valley (Figure 5a), may result from a period of reduced fluvial connectivity with the foreland followed by a re-opening of the outlet (Hilley & Strecker, 2005). A reduced connectivity with the foreland may be related to gravitational deposits blocking the narrow outlet of the valley. However, due to the (a) lack of evidence for gravitational events or landslide deposits, (b) the narrow geometry of the valley downstream, and (c) the presence of a salt diapir cropping out along the SE border of the Tepelenë massif (Figure 4a), we invoke salt tectonics to explain the possibly temporary closure of the Gjirokastër valley. In fact, the closure of the valley may have occurred following the rise of the diapir that, together with the activity of a major dextral strike-slip fault system that bounds the Tepelenë massif to the SE, may have caused a km-long offset, resulting in the interruption of the Gjirokastër River's connection with the Vjosa River (Figure 4a). The formation of a temporary endorheic system may have caused aggradation in the Gjirokastër valley, followed by regressive erosion of the Vjosa river, breaching the barrier and re-opening the Gjirokastër valley to the north. The lack of datable material in the terraces prevents defining a temporal constraint for this deformation.

Additional evidence of drainage reorganisation is found in the internal sector of the orogen, where the coexistence of varying lithologies, alongside the interplay of inherited compressive structures and younger extensional features, has resulted in a more intricate and complex landscape. This is particularly evident in northern Albania, where Gemignani et al. (2022) identified at least two significant river reorganisation events in the Drin River system since the Miocene. Moreover, the effect of tectonics on the drainage is evident in the system of Korça and Devolli basins, where footwall uplift of the NNE-trending Korça normal fault creates the ridge that separates the two alluvial basins (Figure 4b). The presence of the Devoll water gap carved through this ridge indicates that the erosional power of the Devoll River keeps pace with the fault activity, which is responsible for the ongoing growth of the ridge.

Similarly, wind gaps along the drainage divide separating streams flowing into the Burrel and Drin basins represent the remnants of old stream networks that were profoundly changed by tectonics. Stream flow reversal is indicated by the drainage geometry and by the presence of aggradation deposits (Figures 4c and 4d), while river capture is suggested by the steeper western slope of the ridge (Figure 4d), showing intense incision likely due to headward erosion of the currently westward-draining stream. The formation of these aligned wind-gaps was likely driven by the uplift of the mountain ridge during a compressional phase, or by the activity of a normal fault system in a subsequent extensional regime, as suggested by D'Agostino et al. (2022).

Collectively, based on the morphotectonic analysis and the drainage reorganisation, we identify the tectonic contribution of three main deformation styles:

1. Thrust faulting dominated, e.g., in the external ridge, where drainage reorganisation of large rivers appears as a long-lived process;

2. The combination of normal and thrust faulting, as observed particularly in the middle and internal ridges, where tectonics locally influences the drainage by creating topographic relief and causing the formation of features such as wind gaps, water gaps, stream reversal and river captures. This style, where extension overprinted contractional structures, often leading to drainage reorganisation, has been already observed in other case settings, such as the Apennines (e.g., Buttinelli et al., 2018; Clementucci et al., 2024; Lanari et al., 2023).
3. Salt tectonics, which may have contributed to the local drainage reorganisation as observed in the southern part of the external fold-and-thrust belt system, similar to the Zagros mountains (e.g., Mouthereau et al., 2007).

5.2. Analysis of Denudation Rate Variability

5.2.1. Denudation Rates

The analysis of nine basins revealed a considerable variability of denudation rate values, spanning from 0.18 to 1.28 mm/yr. Nevertheless, a general trend of increasing denudation from west to east across the strike of the belt is evident, with higher values located along the middle ridge. We now discuss whether this trend could be caused by (1) former glaciation or inherited glacial landforms, or (2) by landsliding.

1. In formerly glaciated settings, potential bias on cosmogenic nuclide-derived denudation rates may arise due to glacial oversteepening and resulting non-steady state hillslope processes (e.g., Delunel et al., 2020), as well as glacial abrasion and ice shielding, which can reset surface nuclide inventories and delay the re-establishment of steady-state conditions (e.g.,Wittmann et al., 2007). In Albania, several lines of evidence point to past Quaternary glaciations (Hughes, 2004; Hughes et al., 2006; Hughes & Woodward, 2017; Louis, 1926). Specifically, small, spatially limited glacial bodies were present in the region of Lake Ohrid and Prespa (Gromig et al., 2018; Ribolini et al., 2011), potentially affecting basins #02 and #06. In the upper and middle parts of the Vjosa River Pleistocene glaciation (Hughes et al., 2006; Hughes & Woodward, 2017; Leontaritis et al., 2020; Louis, 1926) left clear signatures both in the landscape morphology and in the sedimentary record of river terraces (Mugnier et al., 2024; Woodward et al., 2008) that may have influenced the denudation dynamics of this system (samples #07, #09, #10, #15). Therefore, to better evaluate a possible control, we analyzed the valley morphology of our sampled basins and their mean elevation relative to the ELA (Equilibrium Line Altitude) of the last cold stage in Greece (MIS 5d-MIS 2; mean ELA 2,174 m a.s.l.; Hughes, 2004; Leontaritis et al., 2020) relative to the integration time of the denudation results. All the studied valleys display characteristic V-shape profiles, indicating fluvial incision rather than a glacial imprint, and are located at an elevation below the estimated ELA. Moreover, the integration time of our results is significantly short (<3.5 ka) due to the high denudation rates which, as also suggested by numerical modeling (e.g., Wittmann et al., 2007), promote a rapid return to steady-state conditions following nuclide resetting by glaciation. Therefore, it is reasonable to assume that our basins reached a new post-glacial equilibrium relatively quickly, limiting the influence of glacial coverage on cosmogenic nuclide-derived denudation rates.
2. Overestimation of denudation rates may occur in river systems strongly influenced by landslides due to the decoupling of slope and river processes (Niemi et al., 2005; Ouimet et al., 2009). This is especially relevant in very small catchments (<25 km^2, Niemi et al., 2005; Ouimet et al., 2009) where the impact of individual landslides is less likely to average out over time, potentially leading to an overestimation of denudation rates (Yanites et al., 2009). Thus, it is possible that the particularly high denudation rates of samples #13, #14 and #6 (1.03 ± 0.17, 0.70 ± 0.1, 1.28 ± 0.19 mm/yr, respectively), located in areas where the Albanian flysch is subjected to high gravitational instability, may reflect localized landslide activity rather than broader regional erosion processes. Gravitational slope processes are also observed in other basins (#05 and #09), as revealed by the analysis of recent satellite imagery, but are less pronounced and limited to specific locations along the channels. For instance, basin #09 (0.82 ± 0.1 mm/yr) exhibits signs of instability in the upper part of the catchment, while basin #05 (0.67 ± 0.09 mm/yr) shows sporadic gravitational activity in the lower part of the catchment. However, remote sensing observations and field surveys indicate that all these basins are affected by shallow landslides likely triggered by lithological heterogeneities within the flysch (see, Figure S2 in Supporting Information S1), which contains a high proportion of marl and is therefore more prone to instability and erosion. Moreover, all the sampled landslide-affected basins have areas exceeding 30 km^2, which helps to reduce landslide-related bias by ensuring effective mixing of sediments from steady-state erosion and gravitational processes (Niemi et al., 2005; Ouimet et al., 2009). In addition, erosion linked to calanchi badlands-type morphologies is commonly observed in the marly flysch formations throughout the study region, and thus

represents a typical and regionally relevant erosional mechanism. This interpretation is further supported by the relatively moderate average slopes of these basins (ranging from 18° to 21°, see, Figure S1 in Supporting Information S1), which fall below the hillslope threshold of ∼30° considered the point beyond which erosion rates no longer increase linearly with slope (Ouimet et al., 2009). This threshold corresponds to denudation rates of approximately 0.2–0.25 mm/yr. Our measured rates are significantly higher than these values, yet, we do not observe any deviation from the expected trend of increasing denudation with increasing slope (see, Figure S1 in Supporting Information S1). The normalized channel steepness index (k_{sn}) has proven to be a more reliable predictor of erosion in tectonically active landscapes (Wobus et al., 2006), showing a progressive linear steepening of river channels up to erosion rates of ∼0.6 mm/yr, over the hillslope threshold (Ouimet et al., 2009). However, we do not observe in our samples a clear correlation between k_{sn} and denudation rates (see, Figure S1 in Supporting Information S1). For all these reasons, and given the alignment with the other data, we do not discard samples #6, #13 and #14 but, in order to acknowledge the increased values caused by landslides, we consider them as upper-bound values yielding the maximum apparent denudation rates. In conclusion, we acknowledge that the potential influence of both recent glaciations and landslide activity on our results cannot be entirely ruled out, and could contribute to the elevated denudation rates observed in some catchments, but these processes do not dominate the overall denudation rate signal.

Our data reveal a progressive eastward increase in denudation rates across the strike of the belt. This trend is consistent with the regional increase in incision rates inferred from river terraces (Guzmán et al., 2023, and references therein), as well as with the exhumation patterns of the southern Albanides (Rossetti et al., 2024). Despite the different temporal (>10^6 yrs) and spatial scales covered by thermochronology compared to our denudation rates, the thermochronological data record progressively younger cooling ages toward the hinterland, from middle to late Miocene-Pliocene, suggesting enhanced exhumation in the internal sectors of the orogenic belt. By assuming a constant geothermal gradient of 20°C/km and a nominal closure temperature of about 70°C for AHe (e.g., Reiners & Brandon, 2006), Rossetti et al. (2024) suggest a pulse of 3–4 km of exhumation during the latest Miocene-Pliocene. Since the spatial distribution of cooling ages is inconsistent with the foreland-ward propagation of the shallow fold-and-thrust belt, this pattern has been interpreted as the result of a deeper geodynamic mechanism.

The following sections compare our results with previously published data on river incision rates and low-temperature thermochronology. The available thermochronological data do not directly overlap with our sampled basins, therefore the comparison relies on the geographically closest thermochronological samples to our sampled catchments.

5.2.1.1. External Ridge

Concerning the external ridge, the high denudation rate of sample #14 (0.70 mm/yr) may be explained by the combined effect of the Vorë back thrust and the deep compressive structure responsible for the 2019 Durres earthquake. These structures likely enhanced the uplift in this area, thereby increasing the river's erosional power and, consequently, the observed denudation rate. Moreover, the denudation rate of 0.70 mm/yr matches the long-term (>25 ka) incision rate (0.7 mm/yr), which remains constant also in the short-term (<25 ka), on river terraces calculated by Guzmán (2013) along the Erzen River. Active tectonics in this area is further confirmed by recent data from Guzmán et al. (2023), who dated T1 in the floodplain near the mountain ridge generated by the Vorë back-thrust, to approximately 1.5 ka, suggesting a recent uplift within the last 1.5 ka (Mugnier et al., 2024).

To the south, samples #10 and #15 exhibit lower denudation rates compared to sample #09. Samples #10 and #15 lie on the footwall of two thrust faults (WTT and LTT), while sample #09 is located in the hanging wall of LTT. Although focal mechanisms reveal evidence of both compressional and strike-slip tectonic activity only for the thrust near sample #10 (WTT, cfr. Figures 1c and 6), Guzmán et al. (2013) estimated for the thrust LTT a vertical slip rate of approximately 0.8 mm/yr in the proximity of Lushnje, which decreases to ∼0.2 mm/yr toward the south. This would also explain the high denudation rate value obtained for basin #09 which, with respect to the other two, is surrounded by steep and elevated topography. Guzmán et al. (2013) calculated that long-term incision rates in the middle section of the Vjosa River are higher than in the upper section. Recently, additional ^{14}C data—one from colluvium and one from T5, both in the middle section of the Vjosa River—were incorporated into the data set (Guzmán et al., 2023), revealing an incision rate of approximately 0.9 mm/yr for T5. Sample #2 (0.39 mm/yr), located at the boundary between the external and middle ridges—that is, at the

transition between the compressional and extensional domains—may be reasonably influenced by the activity of the Tomori Thrust (TT), which has an estimated vertical slip rate of ∼0.3 mm/yr (Guzmán et al., 2013). The denudation rate for this sample is also consistent with the short-term (<19 ka) incision rates calculated by Guzmán (2013) for the terraces along the Osum River, which range from 0.7 to 0.8 mm/yr.

While the northern sector of the external ridge is not covered by thermochronological data, the southern sector includes several samples with AHe cooling ages ranging from 6.3 to 3.1 Ma (samples 4–9; Figures 2a and 2b in Rossetti et al., 2024). In this comparison we include also sample 9 from Rossetti et al. (2024) since its location is at the transition between the external and the middle ridges. These cooling ages can be analytically converted into erosion rates (Agetoedot; Willett & Brandon, 2013, see Supporting Information S1), which range from 0.3 to 0.8 mm/yr and are comparable to our denudation rates (samples #02, #09, #10 and #15, 0.39 ± 0.05, 0.82 ± 0.10, 0.25 ± 0.03 and 0.18 ± 0.02 mm/yr, respectively).

5.2.1.2. Middle Ridge

The middle ridge, on the other hand, is characterized by higher denudation values. To the north (Figure 6), the uplift caused by the activity of both the KT fault and the fault bordering the Burrel Basin may have enhanced the river's erosive power in basin #13 by steepening the river profile and contributing to its high denudation rate of 1.03 mm/yr. This rate is slightly higher than the short-term (<25 ka) incision rate calculated by Guzmán (2013) in the Erzen river domain, which is around 0.7 mm/yr. This basin is also located close to recently sampled terrace (T3) in the study by Guzmán et al. (2023), which was dated using ^{14}C and exhibits an incision rate of approximately 0.6 mm/yr. The higher denudation rates can be explained by the morphology of the basin, which appears to be affected by landslides in the fine-grained flysch deposits (see, Figure S2 in Supporting Information S1). Sample #5 lies in a region highly influenced by normal faults of the Elbasan system, which has a vertical slip rate >1 mm/yr (Guzmán et al., 2013), with faults offsetting the terrace T1 at a rate of 1–2 mm/yr over the last 6 ka (Mugnier et al., 2024). This sector of the Devoll River is well represented by dated terraces, which indicate high incision rates, with values reaching up to 1 mm/yr (Guzmán et al., 2013). Recent ^{14}C data on T5 and T7 further confirm this pattern (Guzmán et al., 2023). The Tomori thrust, which has an estimated vertical slip rate of ∼0.3 mm/yr (Guzmán et al., 2013), may have contributed to the high denudation rate observed in basin #6 (1.28 mm/yr), the highest in the region. In this area, the short-term incision rates range from 0.8 to 1 mm/yr for the Devoll river domain (samples #05, #06) (Guzmán et al., 2013, 2023). To the south, the relatively higher denudation rate of 0.48 mm/yr for sample #07 might be attributed to the activity of Konitsa normal fault system, which has a vertical slip rate of >0.4 mm/yr. Beyond the local contributions of these faults, the results obtained appear to be consistent with the short-term (<25 ka), relatively low incision rate of 0.3 mm/yr calculated by Guzmán (2013) in the Vjosa domain. Despite the consistency of our data with the existing literature, it is important to consider the potential influence of the so-called "Sadler effect", first observed in sedimentology, which states that incision rates often appear higher when measured over shorter timescales (Finnegan et al., 2014).

Regarding the middle ridge, thermochronological data are lacking in its northern sector, in contrast to the central and southern sectors. Four thermochronological samples (samples 9 to 12; Figures 2a and 2b in Rossetti et al., 2024) are located in the middle ridge. Specifically, samples 9 and 10 are situated near samples #06, yielding AHe cooling ages between 7.2 and 4.3 Ma. The derived erosion rates (Agetoedot; Willett & Brandon, 2013, see Supporting Information S1) range between 0.3 and 0.6 mm/yr. Conversely, samples 11 and 12 (Figures 2a and 2b in Rossetti et al., 2024) show cooling ages (6 and 3.8 Ma) and slightly higher erosion rates (0.2–0.8 mm/yr). Although not measured in the immediate vicinity of sample #05, these values are nonetheless comparable to its denudation rate (0.67 ± 0.01 mm/yr), but lower than the maximum rate recorded at sample #06 (1.28 ± 0.19 mm/yr). In this case, the bias from shallow landsliding has already been accounted for; however, it is important to note that low-temperature thermochronometers do not capture the very shallow processes, nor signals of active extension if exhumation is too limited (i.e., less than 2–3 km) to be recorded by the AHe system. Further south, thermochronological samples 6 and 7 (4.7–3.1 Ma; Figures 2a and 2b; Rossetti et al., 2024) are the closest to our sample #07. The erosion rates associate with these cooling ages range from 0.3 to 0.8 mm/yr, within the same range as the denudation rate measured for sample #07 (0.48 ± 0.06 mm/yr). Overall, the middle ridge exhibits relatively high erosion rates. The agreement between long- and short-term estimates across different orogenic domains suggests that erosion rates have been relatively high over the last 7–6 million years.

5.3. Causes for Rate Variability

In general, the observed spatial variability in denudation rate could be attributed to several factors, namely (a) lithological variability (e.g., Norton et al., 2011), (b) spatial variation in precipitation and climate (e.g., Bookhagen & Strecker, 2012), (c) drainage reorganisation (Malusá et al., 2024; Prince et al., 2011; Yanites et al., 2013), and (d) base-level changes due to eustatism or rock uplift (Gray et al., 2014; Montgomery & Brandon, 2002).

1. *Lithological Variability*: lithology plays a key role in river incision, as more resistant rock types reduce the erodibility coefficient (K) of the stream power law, leading to lower erosion rates (Whipple & Tucker, 1999). We can exclude lithological variability because all samples are sourced from the same lithotype (i.e., siliciclastic flysch deposits), and the variability in cohesion and resistance among the flysch unit members, ranging from sandier to more marly compositions, is likely negligible.
2. *Precipitation and Climate*: averaged present-day precipitation rates calculated for each basin over a period of 11 years (WorldClim grid database; Fick & Hijmans, 2017). Exhibit similar values ranging from ∼1,090 mm/yr to a maximum of 1,240 mm/yr This leads to the assumption that variability in denudation rates between external and middle ridges is likely not caused by spatial changes in present-day precipitation. Considering the integration time of our samples ($\sim 10^2$–10^3 years), climatic conditions during this period are not expected to have varied significantly between the middle and external ridge domains given their geographical proximity. Furthermore, there is no evidence of substantial differences in precipitation between northern and southern Albania since the Last Glacial Maximum (Wagner et al., 2019), reinforcing the assumption that precipitation variability has not been a major factor in shaping the observed patterns.

From a general perspective, several studies on river terrace sequences have demonstrated how climatic variations have shaped the Albanian landscape, influencing water discharge, sediment supply, and vegetation distribution over the past 200 ka (Carcaillet et al., 2009; Guzmán et al., 2013, 2023; Mugnier et al., 2024; Woodward et al., 2008). Therefore, given the influence of climate on river terrace formation, a similar impact on denudation rates might be expected. However, if climate were the primary driver of denudation rate variability, we would expect a more homogeneous spatial pattern across basins with similar elevation and exposure. Instead, the observed spatial variability of our denudation rates aligns with the spatial variability of incision rates calculated on the terraces, which has been attributed to differential uplift in the Albanian mountains and the local influence of faults (Carcaillet et al., 2009; Guzmán et al., 2013).

3. *Drainage reorganisation*: Sudden shifts in a basin's internal dynamics, such as river capture events, can lead to substantial variations in catchment-wide erosion rates (e.g., Yanites et al., 2013). When a river capture occurs, the capturing river rapidly expands its drainage area, increasing water discharge and sediment flux, which in turn enhances downstream erosion and triggers slope adjustments to establish a new equilibrium (Langbein & Leopold, 1964; Yanites et al., 2013). At the same time, the increased erosional power propagates upstream, driving incision along both the main trunk and its tributaries, as demonstrated by studies on knickpoint migration (Bishop, 1995; Yanites et al., 2013). Although Albania features several documented cases of river capture and drainage integration (e.g., the Drin system; Gemignani et al., 2022; the Shkumbin-Devoll system; Guzmán et al., 2013; Melo, 1961), our sampled basins are not located near any significant capture points, except for the Devoll River capture, documented and dated at ∼6 ka by Guzmán (2013), which may have influenced some of our samples (#02, #05, #06). Our analysis shows no clear indication of an incision wave propagating through the river system from the capture point. In fact, the limited elevation difference (∼20 m) between the captured and capturing rivers seems insufficient to significantly impact the main trunk and its tributaries. Furthermore, basin #05, the closest to the capture point, displays a denudation rate (0.67 ± 0.09 mm/yr) lower than basin #06, which is located farther upstream and has a denudation rate of 1.28 ± 0.19 mm/yr, even though we would expect higher rates for the basin closer to the capture point. Moreover, both basins exhibit longitudinal river profiles in equilibrium, suggesting either that the capture event of the main river is too recent for its effects to have propagated upstream and been fully recorded in the denudation rates; or that the tributaries have already adjusted to the new conditions, which is unlikely given the recent timing of the capture (∼6 ka; Guzmán et al., 2013). This discrepancy between the two denudation rates could be attributed to localized processes such as landsliding (particularly in sample #06) or may still reflect longer-term landscape evolution. Thus, river capture does not appear to be the primary driver of spatial variability in denudation rates.

4. *Base-level change:* Beyond the climatic variations discussed in 2), changes in base level can significantly influence the river erosional capacity (Ballato et al., 2015; Ouimet et al., 2009; Schumm and Scheler, 1993). Base-level fluctuations govern whether a river undergoes incision or aggradation as it seeks to restore equilibrium, with a lowering of the base level typically rejuvenating drainage systems and increasing both erosion and sediment flux (Lane, 1955). The ultimate base level for all drainage systems is the sea and, consequently, alternating lowstands and highstands can substantially reshape river dynamics (Schumm and Scheler, 1993). Sea-level fluctuations have been invoked to explain knickpoint distribution and river terraces in the Tropoja Basin, within the Drin drainage system after the Last Glacial Maximum (~20 ka; Gemignani et al., 2022). Without any tectonic forcing, we would expect the Adriatic sea-level changes to have induced a uniform upstream migration of incision waves along all rivers, leading to comparable denudation rates, particularly in catchments closer to the coast (from north to south: #14, #02, #15, #10). However, our results show a maximum rate difference of ~0.5 mm/yr among these basins, with higher rates in the northern and central regions (#14, #02) compared to the southern one (#15, #10). Additionally, incision rates derived from river terraces exhibit significant variability across the entire Albanian territory, including coastal areas (Guzmán et al., 2013, 2023). Therefore, the available evidence suggests that the spatial variability in denudation rates cannot be solely explained by recent eustatic variations.

Relative base-level changes, controlled by variations in rock uplift (Whipple & Tucker, 1999), can occur at regional or local scales, such as differential movement along fault blocks intersected by rivers (e.g., Montgomery & Brandon, 2002). To constrain the uplift, we chose to sample basins with river profiles in equilibrium, i.e., having balanced erosion and uplift and displaying a concave-upward shape (e.g., Whipple & Tucker, 1999). This pre-condition implies that the marked differences in denudation rates between the middle and external ridges likely reflect spatial variations in uplift rates, as already highlighted in previous studies (Carcaillet et al., 2009; Guzmán et al., 2013, 2023). The morphological evidence of river reorganisation and the marked differences in topography along and across the belt further emphasize the tectonic control on the Albanian landscape. Therefore, rock uplift appears to be the main driver of the strong spatial variability of denudation rates across the investigated regions of the Albanides.

5.4. Spatial Variability and Causes of Uplift

Overall, our denudation rates and river analysis indicate that the middle ridge is eroding/uplifting faster than the external one. This pattern is consistent with previously published fluvial incision rates (Carcaillet et al., 2009; Guzmán et al., 2013, 2023), which infer a maximum regional uplift exceeding 1 mm/yr over the past 200 ka (Guzmán et al., 2013) at the transition from the compressional to the extensional domain (Jouanne et al., 2012; D'Agostino et al., 2020). This trend also seems to persist at present, as indicated by GNSS vertical velocity data (see Serpelloni et al., 2022, their Figure 8a). While the relatively high denudation rates increasing toward the ENE can be sustained by a regional-scale uplift, the good correlation of denudation results with the tectonic structures suggests also a strong local tectonic control, in enhancing the denudation rates. This dual contribution has been already proposed by both Carcaillet et al. (2009) and Guzmán et al. (2013) to justify the regional spatial and temporal variability of incision rates and the local deviations from the regional incision trend.

Our topographic analysis (see swaths in Figures 3, 7a and 7b) confirms this interpretation. In the topographic swath profile shown in Figure 7b and crossing the belt with a WSW-ENE direction, the surface topography appears very irregular and clearly influenced by faulting. However, when filtered at larger spatial windows, the same topography becomes progressively smoother, so that at a wavelength of 12 km the effect of faults on topography is only marginally noticeable, and it disappears completely at 25 km and beyond. In contrast, the elevation difference across the belt is more pronounced to the south (swath B in Figures 3 and 7b) where the topographic bulge reaches its maximum, in the hinterland of the orogen. This geometry persists in the filtered topography across all wavelengths, up to 100 km.

We therefore suggest that the observed spatial variability in denudation/uplift rates and in the distribution of topography may be influenced by both local-scale (shorter wavelength) and regional-scale (longer wavelength) processes. Local-scale deformation, driven primarily by surface faulting, increases denudation rates and, consequently, uplift rates, through the movement of fault blocks. Movement along these normal and thrust faults induces localized uplift in the footwall and hanging-wall regions, respectively, and contributes to ridge growth, affecting the drainage pattern and the denudation rates. This spatially variable denudation pattern thus reflects the

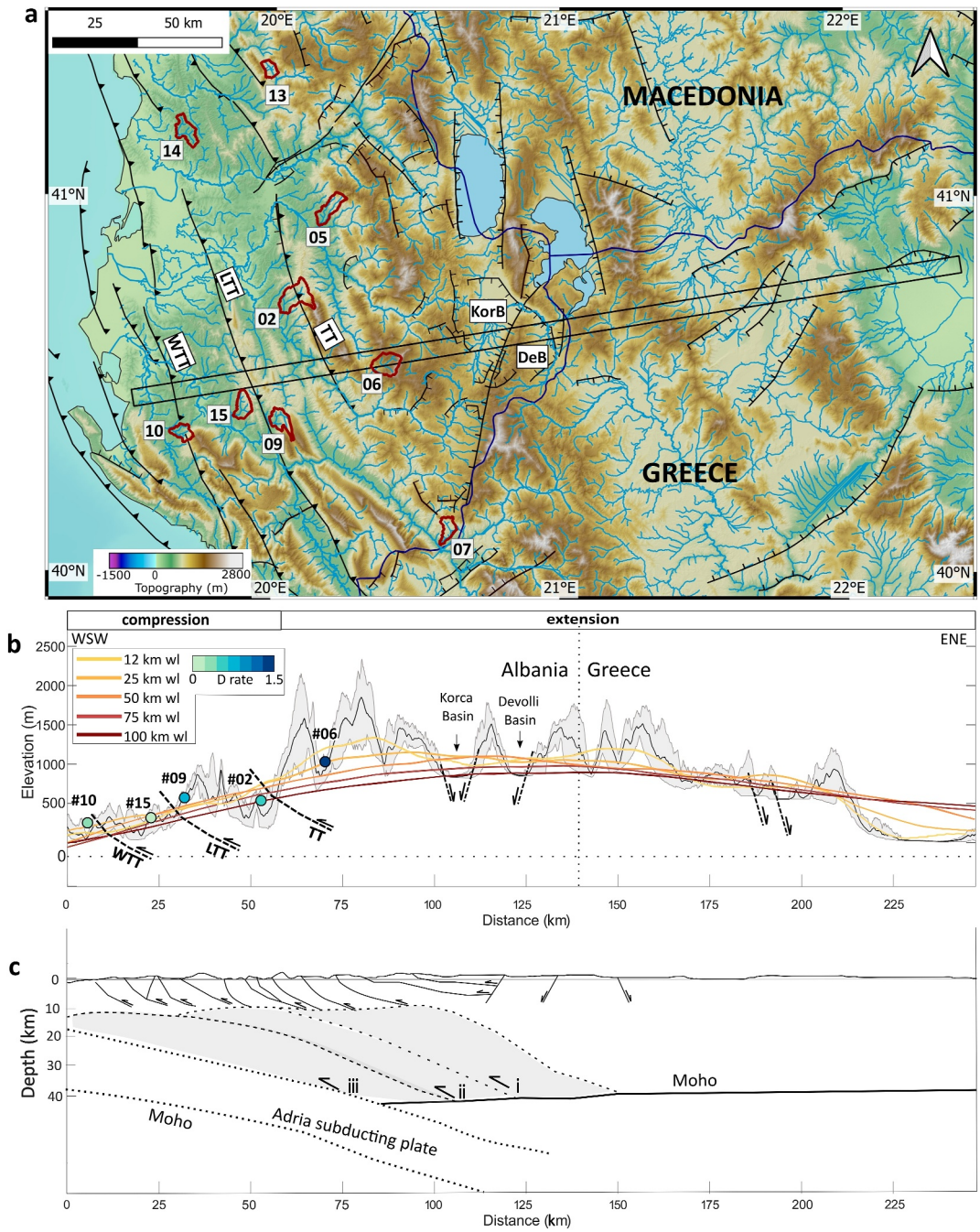

Figure 7. (a) Topographic-tectonic-drainage map showing the sampled basins as red polygons and the trace of the WSW-ENE swath profile crossing Albania and Greece. (b) Topographic swath profile illustrating the mean (black), maximum and minimum (gray) topography. Along the swath profile the main tectonic structures, the averaged denudation rates of the crossed basins (shown as color-coded dots according to their values) and the filtered topography at different wavelengths are shown. (c) Schematic model of crustal underplating process (after Rossetti et al., 2024).

heterogeneous distribution of tectonic deformation across the study area. The deep-seated mechanisms driving regional-scale deformation cannot be defined with our data. However, the long-wavelength signal resulting from the topographic analysis, combined with the increase in denudation rates across the strike of the belt, appears to be consistent with the regional incision pattern (Carcaillet et al., 2009; Guzmán et al., 2013, 2023) and the long-term (10^6 yrs) exhumation pattern (i.e., from the latest Miocene-Pliocene for Albania, Rossetti et al., 2024; and possibly earlier for the more internal orogenic domains of the Hellenides) identified by thermochronological

studies (Rossetti et al., 2024). Deep crustal underplating has been proposed as a plausible mechanism driving regional uplift (Figure 7c; Rossetti et al., 2024), and the consistency of our results with the existing thermochronological and river incision framework suggests that the long-term signal captured in our analysis may still be shaping the landscape today.

6. Conclusions

In this study, we investigated the tectonic imprint on the landscape of the Albanides, presenting the first basin averaged ^{10}Be-derived denudation rates in conjunction with topographic and river network analysis for the region. Denudation rates, derived from nine quartz-bearing basins distributed across the middle and the external ridges, exhibit significant variability, ranging from 0.18 to 1.28 mm/yr. The magnitude of these rates suggests that the orogen is undergoing relatively rapid erosion, and their spatial distribution, together with evidence of river network reorganisation, reveals a strong correlation with active tectonic structures.

In the external compressional domain, denudation rates are influenced predominantly by thrust fault activity, whereas in the middle ridge higher denudation rates correspond roughly to the transition zone from compressional to extensional regimes, reflecting the effect of normal faulting and associated uplift. Given that the sampled basins were selected based on the assumption of equilibrium in river longitudinal profiles, it is reasonable to infer that the spatial variability in denudation rates likely reflects a spatial variability in uplift rates. Additionally, the combined evidence of geomorphological features such as wind and water gaps, river terraces, and river network reorganisation indicates that the landscape of the Albanides is actively responding to spatial variations in uplift rate.

We conclude that the main mechanisms of deformation include a combination of local and regional processes, as already proposed in previous studies (e.g., Carcaillet et al., 2009; Guzmán et al., 2013). At the regional scale and over longer timescales (10^6 years), deep processes, such as underplating, likely drive the broad uplift pattern that defines the modern orogen topography. At the local scale, upper crust normal faults, active in the internal domain, and thrust faults in both domains, influence the denudation variability and contribute to spatial differences in uplift rates, which mirror the tectonic heterogeneity of this region.

This study demonstrates how the integration of geomorphological, thermochronological and cosmogenic denudation data strengthens the existing framework for quantifying spatial and temporal distribution of uplift in the Albanides. The consistency of our denudation rates with long-term (10^6 yrs), long-wavelength thermochronological studies and short-term (<200 ka) river incision rates provides further reliability to our data. To better quantify uplift in the Albanides, future research should target areas of the belt where the absence of quartz prevents the use of in situ cosmogenic methods, by applying lithology-independent techniques such as meteoric ^{10}Be/^{9}Be.

Acknowledgments
This research was supported by the MUR (Ministry of University and Research), Excellence Department Initiative, Art. 1, com. 314–337, Low 232/2016, and by PRIN 2017–2020 (Geodynamics of the Arabia-Eurasia collisional zones, PI C. Faccenna). We thank the Editor, Djordje Grujic, for handling this manuscript and providing valuable feedback, and the reviewers, Ariane Binnie and the anonymous reviewer, for their constructive comments that significantly improved this work. We thank the technicians of the Earth Surface Geochemistry Section 3.3 at GFZ Helmholtz Centre for Geosciences for the assistance in the laboratory procedures. We thank the Professors of the Polytechnic University of Tirana, Prof. Bardhyl Muceku and Prof. Cercis Durmishi, for guiding and supporting us with their expertise in all the field campaigns in Albania. We thank Dr. Riccardo Reitano, Dr. Romano Clementucci and Dr. Riccardo Lanari for their fundamental support in the river analysis. Open Access funding enabled and organized by Projekt DEAL.

Data Availability Statement

We provide online supplementary material in the Supporting Information S1 file, which includes a simplified overview of the stream power law and knickpoint analysis to support the drainage network analysis, additional information on the in situ ^{10}Be cosmogenic technique, and supplementary results. The data are also stored and available for download from the Zenodo repository ("Building Topography in a Continental Subduction Orogen: Insights from Geomorphic Analysis and ^{10}Be Denudation Rates of the Albanides"; https://doi.org/10.5281/zenodo.15244016).

References

Albanian Geological Survey. (2002). Geological Map of Albania 1: 200 000 scale.

Aliaj, S. (1994). Nappes structures in Southeastern Albania= Τεκτονιή των καλλυμάτων στην NA Αλβανία. *Δελτίον της Ελληνικής Γεωλογικής Εταιρίας*, *30*(2), 459–466.

Aliaj, S. (1998). Neotectonic structure of Albania. https://www.researchgate.net/publication/345433372

Aliaj, S., Baldassarre, G., & Shkupi, D. (2001). Quaternary subsidence zones in Albania: Some case studies. In *Bulletin of Engineering Geology and the Environment* (Vol. 59(4), pp. 313–318). https://doi.org/10.1007/s100640000063, Springer-Verlag.

Argnani, A. (2013). The influence of Mesozoic palaeogeography on the variations in structural style along the front of the Albanide thrust-and-fold belt. *Italian Journal of Geosciences*, *132*(2), 175–185. https://doi.org/10.3301/IJG.2012.02

Balco, G., Stone, J. O., Lifton, N. A., & Dunai, T. J. (2008). A complete and easily accessible means of calculating surface exposure ages or erosion rates from ^{10}Be and ^{26}Al measurements. *Quaternary Geochronology*, *3*(3), 174–195. https://doi.org/10.1016/j.quageo.2007.12.001

Balek, J. (1966). Hydrological regimes of Albania Rivers. *Hydrological Sciences Journal*, *11*(2), 69–75. https://doi.org/10.1080/02626666609493459

Ballato, P., Landgraf, A., Schildgen, T. F., Stockli, D. F., Fox, M., Ghassemi, M. R., et al. (2015). The growth of a Mountain belt forced by base-level fall: Tectonics and surface processes during the evolution of the Alborz Mountains, N Iran. *Earth and Planetary Science Letters*, *425*, 204–218. https://doi.org/10.1016/j.epsl.2015.05.051

Basili, R., Kastelic, V., Demircioglu Tumsa, M. B., Garcia Moreno, D., Nemser, E. S., Petricca, P., et al. (2013). European Database of Seismogenic Faults (EDSF) [Dataset]. *Istituto Nazionale di Geofisica e Vulcanologia (INGV)*. https://doi.org/10.6092/ingv.it-share-edsf

Binnie, S. A., Phillips, W. M., Summerfield, M. A., & Keith Fifield, L. (2006). Sediment mixing and basin-wide cosmogenic nuclide analysis in rapidly eroding mountainous environments. *Quaternary Geochronology*, *1*(1), 4–14. https://doi.org/10.1016/j.quageo.2006.06.013

Bishop, P. (1995). 449-Drainage rearrangement by river capture, beheading and diversion. *Progress in Physical Geography: Earth and Environment*, *19*(4), 449–473. https://doi.org/10.1177/030913339501900402

Bookhagen, B., & Strecker, M. R. (2012). Spatiotemporal trends in erosion rates across a pronounced rainfall gradient: Examples from the southern central Andes. *Earth and Planetary Science Letters*, *327–328*, 97–110. https://doi.org/10.1016/j.epsl.2012.02.005

Borchers, B., Marrero, S., Balco, G., Caffee, M., Goehring, B., Lifton, N., et al. (2016). Geological calibration of spallation production rates in the CRONUS-Earth project. *Quaternary Geochronology*, *31*, 188–198. https://doi.org/10.1016/j.quageo.2015.01.009

Božović, M., Prelević, D., Romer, R. L., Barth, M., Van Den Bogaard, P., & Boev, B. (2013). The Demir Kapija Ophiolite, Macedonia (FYROM): A snapshot of subduction initiation within a back-arc. *Journal of Petrology*, *54*(7), 1427–1453. https://doi.org/10.1093/petrology/egt017

Braun, J. (2003). Pecube: A new finite-element code to solve the 3D heat transport equation including the effects of a time-varying, finite amplitude surface topography. *Computers & Geosciences*, *29*(6), 787–794. https://doi.org/10.1016/S0098-3004(03)00052-9

Brombin, V., Barbero, E., Saccani, E., Precisvalle, N., Lepitkova, S., Milevski, I., et al. (2022). Subduction signature of the Vardar ophiolite of North Macedonia: New constraints from geochemical and stable isotope data. *Ofioliti*, *47*(2), 1–54. https://doi.org/10.4454/ofioliti.v47i2.553

Burchfiel, B. C., Nakov, R., Dumurdzanov, N., Papanikolaou, D., Tzankov, T., Serafimovski, T., et al. (2008). Evolution and dynamics of the Cenozoic tectonics of the South Balkan extensional system. *Geosphere*, *4*(6), 919–938. https://doi.org/10.1130/GES00169.1

Burchfiel, B. C., Royden, L. H., Papanikolaou, D., & Pearce, F. D. (2018). Crustal development within a retreating subduction system: The Hellenides. *Geosphere*, *14*(3), 1119–1130. https://doi.org/10.1130/GES01573.1

Buttinelli, M., Pezzo, G., Valoroso, L., De Gori, P., & Chiarabba, C. (2018). Tectonics inversions, fault segmentation, and triggering mechanisms in the central Apennines normal fault system: Insights from high-resolution velocity models. *Tectonics*, *37*(11), 4135–4149. https://doi.org/10.1029/2018TC005053

Carcaillet, J., Mugnier, J. L., Koçi, R., & Jouanne, F. (2009). Uplift and active tectonics of southern Albania inferred from incision of alluvial terraces. *Quaternary Research*, *71*(3), 465–476. https://doi.org/10.1016/j.yqres.2009.01.002

Cermak, V., Kresl, M., Kucerová, L., Safanda, J., Frasheri, A., Kapedani, N., et al. (1996). Heat flow in Albania. *Geothermics*, *25*(1), 91–102. https://doi.org/10.1016/0375-6505(95)00036-4

Clementucci, R., Lanari, R., Faccenna, C., Crosetto, S., Reitano, R., Zoppis, G., & Ballato, P. (2024). Morpho-tectonic evolution of the Southern Apennines and Calabrian arc: Insights from Pollino range and surrounding extensional intermontane basins. *Tectonics*, *43*(5). https://doi.org/10.1029/2023TC008002

Copley, A., Boait, F., Hollingsworth, J., Jackson, J., & McKenzie, D. (2009). Subparallel thrust and normal faulting in Albania and the roles of gravitational potential energy and rheology contrasts in Mountain belts. *Journal of Geophysical Research*, *114*(5). https://doi.org/10.1029/2008JB005931

Crameri, F., Lithgow-Bertelloni, C. R., & Tackley, P. J. (2017). The dynamical control of subduction parameters on surface topography. *Geochemistry, Geophysics, Geosystems*, *18*(4), 1661–1687. https://doi.org/10.1002/2017GC006821

D'agostino, N., Copley, A., Jackson, J., Koçi, R., Hajrullai, A., Duni, L., & Kuka, N. (2022). Active tectonics and fault evolution in the Western Balkans. *Geophysical Journal International*, *231*(3), 2102–2126. https://doi.org/10.1093/gji/ggac316

D'Agostino, N., Métois, M., Koci, R., Duni, L., Kuka, N., Ganas, A., et al. (2020). Active crustal deformation and rotations in the Southwestern Balkans from continuous GPS measurements. *Earth and Planetary Science Letters*, *539*, 116246. https://doi.org/10.1016/j.epsl.2020.116246

Delunel, R., Schlunegger, F., Valla, P. G., Dixon, J., Glotzbach, C., Hippe, K., et al. (2020). Late-Pleistocene catchment-wide denudation patterns across the European Alps. In *Earth-Science Reviews* (Vol. 211, p. 103407), Elsevier B.V. https://doi.org/10.1016/j.earscirev.2020.103407

Dewald, A., Heinze, S., Jolie, J., Zilges, A., Dunai, T., Rethemeyer, J., et al. (2013). CologneAMS, a dedicated center for accelerator mass spectrometry in Germany. *Nuclear Instruments and Methods in Physics Research Section B: Beam Interactions with Materials and Atoms*, *294*, 18–23. https://doi.org/10.1016/j.nimb.2012.04.030

Dodson, M. I. (1973). Closure temperature in cooling geochronological and petrological systems. In *Contributions to Mineralogy and Petrology* (Vol. 40(3), 259–274). https://doi.org/10.1007/bf00373790, Springer-Verlag.

Dufaure, J.-J., Fouache, E., & Denèfle, M. (1999). Tectonique et évolution géomorphologique: L'exemple du bassin de Korçë (Albanie)/Tectonics and geomorphological evolution: The example of the Korçë basin (Albania). *Géomorphologie: Relief, Processus, Environnement*, *5*(2), 111–128. https://doi.org/10.3406/morfo.1999.982

England, P., & Molnar, P. (1990). Surface uplift, uplift of rocks, and exhumation of rocks. *Geology*, *18*(12), 1173. https://doi.org/10.1130/0091-7613(1990)018<1173:suuora>2.3.co;2

Ernst, W. G. (2010). Subduction-zone metamorphism, Calc-alkaline magmatism, and convergent-margin crustal evolution. *Gondwana Research*, *18*(1), 8–16. https://doi.org/10.1016/j.gr.2009.05.010

Faccenna, C., & Becker, T. W. (2020). Topographic expressions of mantle dynamics in the Mediterranean. In *Earth-Science Reviews* (Vol. 209). 103327, Elsevier B.V. https://doi.org/10.1016/j.earscirev.2020.103327

Faccenna, C., Becker, T. W., Auer, L., Billi, A., Boschi, L., Brun, J. P., et al. (2014). Mantle dynamics in the Mediterranean. *Reviews of Geophysics*, *52*(3), 283–332. https://doi.org/10.1002/2013RG000444

Feriozzi, F., Siravo, G., & Speranza, F. (2025). Heritage of Tethyan Oceanic transform faults within alpine orogens: Paleomagnetic evidence from the Shkoder-Peja transverse zone (Northern Albania). *Tectonics*, *44*(6), e2024TC008743. https://doi.org/10.1029/2024TC008743

Fick, S. E., & Hijmans, R. J. (2017). WorldClim 2: New 1-km spatial resolution climate surfaces for global land areas. *International Journal of Climatology*, *37*(12), 4302–4315. https://doi.org/10.1002/joc.5086

Finnegan, N. J., Schumer, R., & Finnegan, S. (2014). A signature of transience in bedrock river incision rates over timescales of 10 4–10 7 years. *Nature*, *505*(7483), 391–394. https://doi.org/10.1038/nature12913

Forte, A. M., & Whipple, K. X. (2019). Short communication: The Topographic Analysis Kit (TAK) for Topo Toolbox. *Earth Surface Dynamics*, *7*(1), 87–95. https://doi.org/10.5194/esurf-7-87-2019

Francke, A., Wagner, B., Just, J., Leicher, N., Gromig, R., Baumgarten, H., et al. (2016). Sedimentological processes and environmental variability at Lake Ohrid (Macedonia, Albania) between 637 ka and the present. *Biogeosciences*, *13*(4), 1179–1196. https://doi.org/10.5194/bg-13-1179-2016

Frasheri, A., Bushati, S., & Bare, V. (2009). Geophysical outlook on structure of the Albanides. *Journal of the Balkan Geophysical Society*, *12*(1).

Gasperini, D., Blichert-Toft, J., Bosch, D., Del Moro, A., Macera, P., & Albarède, F. (2002). Upwelling of deep mantle material through a plate window: Evidence from the geochemistry of Italian basaltic volcanics. *Journal of Geophysical Research*, *107*(B12). https://doi.org/10.1029/2001jb000418

Gautheron, C., Tassan-Got, L., Barbarand, J., & Pagel, M. (2009). Effect of alpha-damage annealing on apatite (U-Th)/He thermochronology. *Chemical Geology*, *266*(3–4), 157–170. https://doi.org/10.1016/j.chemgeo.2009.06.001

Gemignani, L., Mittelbach, B. V., Simon, D., Rohrmann, A., Grund, M. U., Bernhardt, A., et al. (2022). Response of drainage pattern and Basin evolution to tectonic and climatic changes along the Dinarides-Hellenides orogen. *Frontiers in Earth Science*, *10*. https://doi.org/10.3389/feart.2022.821707

Granger, D. E., Kirchner, J. W., & Finkel, R. (1996). Spatially averaged long-term erosion rates measured from in situ-produced cosmogenic nuclides in alluvial sediment. *The Journal of Geology*, *104*(3), 249–257. https://doi.org/10.1086/629823

Gray, H. J., Owen, L. A., Dietsch, C., Beck, R. A., Caffee, M. A., Finkel, R. C., & Mahan, S. A. (2014). Quaternary landscape development, alluvial fan chronology and 1 erosion of the Mecca Hills at the southern end of the San Andreas 2 fault zone. https://www.sciencedirect.com/science/article/pii/S0277379114003515

Gromig, R., Mechernich, S., Ribolini, A., Wagner, B., Zanchetta, G., Isola, I., et al. (2018). Evidence for a Younger Dryas deglaciation in the Galicica Mountains (FYROM) from cosmogenic 36Cl. *Quaternary International*, *464*, 352–363. https://doi.org/10.1016/j.quaint.2017.07.013

Grund, M. U. (2023). The Shkoder Peja normal fault system at the Dinaric-Hellenic Junction: A structural and thermochronological study. PhD Thesis. https://doi.org/10.17169/refubium-38273

Guzmán, O. (2013). Chronologie et dynamique de la formation des terrasses fluviales dans des chaînes des montagnes avec une surrection modéré: l'exemple du Vénézuéla et de l'Albanie (PhD thesis). Université de Grenoble. https://tel.archives-ouvertes.fr/tel-00934484

Guzmán, O., Mugnier, J. L., Vassallo, R., Koçi, R., Carcaillet, J., & Jouanne, F. (2023). Fluvial terrace formation in mountainous areas: (1) influence of climate changes during the last glacial cycle in Albania. *Comptes Rendus Geoscience*, *355*, 331–353. https://doi.org/10.5802/crgeos.251

Guzmán, O., Mugnier, J. L., Vassallo, R., Koçi, R., & Jouanne, F. (2013). Vertical slip rates of active faults of southern Albania inferred from river terraces. *Annals of Geophysics*, *56*(6). https://doi.org/10.4401/ag-6218

Hack, J. T. (1957). Studies of longitudinal stream profiles in Virginia and Maryland (Vol. *294*). US Government Printing Office.

Handy, M. R., Giese, J., Schmid, S. M., Pleuger, J., Spakman, W., Onuzi, K., & Ustaszewski, K. (2019). Coupled crust-mantle response to slab tearing, bending, and rollback along the Dinaride-Hellenide orogen. *Tectonics*, *38*(8), 2803–2828. https://doi.org/10.1029/2019TC005524

Handy, M. R., Ustaszewski, K., & Kissling, E. (2015). Reconstructing the alps–Carpathians–Dinarides as a key to understanding switches in subduction polarity, slab gaps and surface motion. *International Journal of Earth Sciences*, *104*(1), 1–26. Springer Verlag. https://doi.org/10.1007/s00531-014-1060-3

Hilley, G. E., & Strecker, M. R. (2005). Processes of oscillatory basin filling and excavation in a tectonically active orogen: Quebrada Del Toro Basin, NW Argentina. *Bulletin of the Geological Society of America*, *117*(7–8), 887–901. https://doi.org/10.1130/B25602.1

Hoffmann, N., Reicherter, K., Fernández-Steeger, T., & Grützner, C. (2010). Evolution of ancient Lake Ohrid: A tectonic perspective. *Biogeosciences*, *7*(10), 3377–3386. https://doi.org/10.5194/bg-7-3377-2010

Howard, A. D., & Kerby, G. (1983). Channel changes in badlands. *Geological Society of America Bulletin*, *94*(6), 739–752. https://doi.org/10.1130/0016-7606(1983)94<739:ccib>2.0.co;2

Hughes, P. D. (2004). Quaternary glaciation in the Pindus Mountains, Northwest Greece. Apollo - University of Cambridge Repository. https://doi.org/10.17863/CAM.20476

Hughes, P. D. (2007). Recent behaviour of the Debeli namet Glacier, durmitor, Montenegro. *Earth Surface Processes and Landforms*, *32*(10), 1593–1602. https://doi.org/10.1002/esp.1537

Hughes, P. D. (2009). Twenty-first century glaciers and climate in the Prokletije Mountains, Albania. *Arctic Antarctic and Alpine Research*, *41*(4), 455–459. https://doi.org/10.1657/1938-4246-41.4.455

Hughes, P. D., & Woodward, J. C. (2017). Quaternary glaciation in the Mediterranean Mountains: A new synthesis. *Geological Society, London, Special Publications*, *433*(1), 1–23. https://doi.org/10.1144/sp433.14

Hughes, P. D., Woodward, J. C., & Gibbard, P. L. (2006). Quaternary glacial history of the Mediterranean Mountains. *Progress in Physical Geography*, *30*(3), 334–364. https://doi.org/10.1191/0309133306pp481ra

Johnson, M. R., & Harley, S. L. (2012). *Orogenesis: The making of Mountains*. Cambridge University Press.

Jolivet, L., & Brun, J. P. (2010). Cenozoic geodynamic evolution of the Aegean. *International Journal of Earth Sciences*, *99*(1), 109–138. https://doi.org/10.1007/s00531-008-0366-4

Jolivet, L., Faccenna, C., Goffe, B., Burov, E., & Agard, P. (2003). Subduction tectonics and exhumation of high-pressure metamorphic rocks in the Mediterranean orogens. *American Journal of Science*, *303*(5), 353–409. https://doi.org/10.2475/ajs.303.5.353

Jolivet, L., Menant, A., Clerc, C., Sternai, P., Bellahsen, N., Leroy, S., et al. (2018). Extensional crustal tectonics and crust-mantle coupling, a view from the geological record. In *Earth-Science Reviews* (Vol. 185, pp. 1187–1209). Elsevier B.V. https://doi.org/10.1016/j.earscirev.2018.09.010

Jouanne, F., Mugnier, J. L., Koci, R., Bushati, S., Matev, K., Kuka, N., et al. (2012). GPS constraints on current tectonics of Albania. *Tectonophysics*, *554–557*, 50–62. https://doi.org/10.1016/j.tecto.2012.06.008

Kilias, A. (2024). The Alpine geological history of the Hellenides from the Triassic to the present—compression vs. extension, a dynamic pair for orogen structural configuration: A synthesis. *Geosciences (Switzerland) Multidisciplinary Digital Publishing Institute (MDPI)*, *14*(Issue 1), 10. https://doi.org/10.3390/geosciences14010010

Kilias, A., Tranos, M., Mountrakis, D., Shallo, M., Marto, A., & Turku, I. (2001). Geometry and kinematics of deformation in the Albanian orogenic belt during the Tertiary. *Journal of Geodynamics*, *31*(2), 169–187. https://doi.org/10.1016/s0264-3707(00)00026-0. http://www.elsevier.nl/locate/jgeodyn

Kirby, E., & Whipple, K. (2001). Quantifying differential rock-uplift rates via stream profile analysis. *Geology*, *29*(5), 415. https://doi.org/10.1130/0091-7613(2001)029<0415:qdrurv>2.0.co;2.http://pubs.geoscienceworld.org/gsa/geology/article-pdf/29/5/415/3521633/i0091-7613-29-5-415.pdf

Kirby, E., & Whipple, K. X. (2012). Expression of active tectonics in erosional landscapes. *Journal of Structural Geology*, *44*, 54–75. https://doi.org/10.1016/j.jsg.2012.07.009

Kissel, C., Speranza, F., & Milicevic, V. (1995). Paleomagnetism of external southern and central Dinarides and northern Albanides: Implications for the Cenozoic activity of the Scutari-pec transverse zone. *Journal of Geophysical Research*, *100*(B8), 14999–15007. https://doi.org/10.1029/95jb01243

Kissling, E. (2024). Adria microplate: A puzzling key stone in west-central Mediterranean geodynamics. *Annals of Geophysics*, *67*(4), G431. https://doi.org/10.4401/ag-9160

Koçi, R., Dushi, E., Begu, E., & Bozo, R. (2018). Impact of tectonics on Rivers terraces geomorphology. *Albania*. https://doi.org/10.5593/sgem2018/1.1

Lacombe, O., Malandain, J., Vilasi, N., Amrouch, K., & Roure, F. (2009). From paleostresses to paleoburial in fold-thrust belts: Preliminary results from calcite twin analysis in the Outer Albanides. *Tectonophysics*, *475*(1), 128–141. https://doi.org/10.1016/j.tecto.2008.10.023

Lal, D. (1991). Cosmic ray labeling of erosion surfaces: In situ nuclide production rates and erosion models. *Earth and Planetary Science Letters*, *104*(2–4), 424–439. https://doi.org/10.1016/0012-821x(91)90220-c

Lanari, R., Reitano, R., Faccenna, C., Agostinetti, N. P., & Ballato, P. (2023). Surface and crustal response to deep subduction dynamics: Insights from the Apennines, Italy. *Tectonics*, *42*(3). https://doi.org/10.1029/2022TC007461

Lane, E. W. (1955). *A study of the shape of channels formed by natural streams flowing in erodible material (No. 9)*. US Army Engineer Division, Missouri River.

Langbein, W. B., & Leopold, L. B. (1964). Quasi-equilibrium states in channel morphology. *American Journal of Science*, *262*(6), 782–794. https://doi.org/10.2475/ajs.262.6.782

Le Goff, J. (2015). Evolution tectono-sédimentaire du système carbonaté "Plateforme Apulienne-Bassin Ionien" au Crétacé supérieur dans le sud de l'Albanie: faciès, géométries, diagénèse et propriétés réservoirs associées. https://theses.hal.science/tel-01278940v1

Leontaritis, A. D., Kouli, K., & Pavlopoulos, K. (2020). The glacial history of Greece: A comprehensive review. *Mediterranean Geoscience Reviews*, *2*(1), 65–90. https://doi.org/10.1007/s42990-020-00021-w

Lewin, J., Macklin, M., & Woodward, J. C. (1991). Late Quaternary fluvial sedimentation in the Voidomatis Basin, Epirus, Northwest Greece. *Quaternary Research*, *35*(1), 103–115. https://doi.org/10.1016/0033-5894(91)90098-p

Lindhorst, K., Krastel, S., Reicherter, K., Stipp, M., Wagner, B., & Schwenk, T. (2015). Sedimentary and tectonic evolution of Lake Ohrid (Macedonia/Albania). *Basin Research*, *27*(1), 84–101. https://doi.org/10.1111/bre.12063

Louis, H. (1926). Glazialmorphologishche Beobachtungen im albanischen Epirus. *Zeitschrift der Gesellschaft für Erdkunde*, 398–409.

Macera, P., Gasperini, D., Piromallo, C., Blichert-Toft, J., Bosch, D., Del Moro, A., & Martin, S. (2003). Geodynamic implications of deep mantle upwelling in the source of Tertiary volcanics from the Veneto region (South-Eastern Alps). *Journal of Geodynamics*, *36*(5), 563–590. https://doi.org/10.1016/j.jog.2003.08.004

Macklin, M. G., Fuller, I. C., Lewin, J., Maas, G. S., Passmore, D. G., Rose, J., et al. (2002). Correlation of fluvial sequences in the Mediterranean Basin over the last 200 ka and their relationship to climate change. *Quaternary Science Reviews*, *21*(14–15), 1633–1641. https://doi.org/10.1016/s0277-3791(01)00147-0

Malusà, M. G., Resentini, A., & Wittmann, H. (2024). Impact of river capture on erosion rates and offshore sedimentation revealed by geological and in situ 10Be cosmogenic data (Corsica, Western Mediterranean). *Earth and Planetary Science Letters*, *637*, 118728. https://doi.org/10.1016/j.epsl.2024.118728

Mazzoli, S., Basilici, M., Spina, V., Pierantoni, P. P., & Tondi, E. (2022). Space and time variability of Detachment- versus ramp-dominated thrusting: Insights from the outer Albanides. *Tectonics*, *41*(8). https://doi.org/10.1029/2022TC007274

Mazzoli, S., D'Errico, M., Aldega, L., Corrado, S., Invernizzi, C., Shiner, P., & Zattin, M. (2008). Tectonic burial and "young" (<10 Ma) exhumation in the southern Apennines fold-and-thrust belt (Italy). *Geology*, *36*(3), 243–246. https://doi.org/10.1130/G24344A.1

Meço, S., & Aliaj, S. (2000). *Geology of Albania, Beiträgezur regionalen Geologie der Erde*. Gebrueder Borntraeger.

Melo, V. (1961). *Neotectonic in the Elbasan-Peqin area from Shkumbin terraces –. Bul*. University. Sht Shkencave Natyrore II. (in Albanian).

Montgomery, D. R., & Brandon, M. T. (2002). Topographic controls on erosion rates in tectonically active Mountain ranges. *Cyaan Magenta Geel Zwart Earth and Planetary Science Letters*, *6273*. www.elsevier.com/locate/epsl

Mouthereau, F., Tensi, J., Bellahsen, N., Lacombe, O., De Boisgrollier, T., & Kargar, S. (2007). Tertiary sequence of deformation in a thin-skinned/thick-skinned collision belt: The Zagros folded belt (Fars, Iran). *Tectonics*, *26*(5). https://doi.org/10.1029/2007TC002098

Muceku, B., Mascle, G. H., & Tashko, A. (2006). First results of fission-track thermochronology in the Albanides. *Geological Society, London, Special Publications*, *260*(1), 539–556. https://doi.org/10.1144/gsl.sp.2006.260.01.23.http://sp.lyellcollection.org/

Muceku, B., Van Der Beek, P., Bernet, M., Reiners, P., Mascle, G., & Tashko, A. (2008). Thermochronological evidence for Mio-Pliocene late orogenic extension in the north-eastern Albanides (Albania). *Terra Nova*, *20*(3), 180–187. https://doi.org/10.1111/j.1365-3121.2008.00803.x

Mugnier, J. L., Guzmán, O., Vassallo, R., Matraku, K., & Jouanne, F. (2024). Fluvial terrace formation in a mountainous area (2): Influence of Eustatism, tectonics and altitudinal distribution of watersheds based on an allostratigraphic study (Albania). *Comptes Rendus Geoscience*, *356*(G1), 211–230. https://doi.org/10.5802/crgeos.278

Niemi, N. A., Oskin, M., Burbank, D. W., Heimsath, A. M., & Gabet, E. J. (2005). Effects of bedrock landslides on cosmogenically determined erosion rates. *Earth and Planetary Science Letters*, *237*(3–4), 480–498. https://doi.org/10.1016/j.epsl.2005.07.009

Nieuwland, D. A., Oudmayer, B. C., & Valbona, U. (2001). The tectonic development of Albania: Explanation and prediction of structural styles. *Marine and Petroleum Geology*, *18*(1), 161–177. https://doi.org/10.1016/s0264-8172(00)00043-x. http://www.elsevier.com/locate/marpetgeo

Nishiizumi, K., Imamura, M., Caffee, M. W., Southon, J. R., Finkel, R. C., & McAninch, J. (2007). Absolute calibration of 10Be AMS standards. *Nuclear Instruments and Methods in Physics Research Section B: Beam Interactions with Materials and Atoms*, *258*(2), 403–413. https://doi.org/10.1016/j.nimb.2007.01.297

Norton, K. P., von Blanckenburg, F., DiBiase, R., Schlunegger, F., & Kubik, P. W. (2011). Cosmogenic 10Be-derived denudation rates of the Eastern and Southern European Alps. *International Journal of Earth Sciences*, *100*(5), 1163–1179. https://doi.org/10.1007/s00531-010-0626-y

Nowack, E. (1921). A contribution to the geography of Albania. *Source: Geographical Review*, *11*(4), 503. https://doi.org/10.2307/208248

Ott, R. F., Gallen, S. F., Caves Rugenstein, J. K., Ivy-Ochs, S., Helman, D., Fassoulas, C., et al. (2019). Chemical versus mechanical denudation in meta-clastic and carbonate bedrock catchments on Crete, Greece, and mechanisms for steep and high carbonate topography. *Journal of Geophysical Research: Earth Surface*, *124*(12), 2943–2961. https://doi.org/10.1029/2019JF005142

Ouimet, W. B., Whipple, K. X., & Granger, D. E. (2009). Beyond threshold hillslopes: Channel adjustment to base-level fall in tectonically active Mountain ranges. *Geology*, *37*(7), 579–582. https://doi.org/10.1130/G30013A.1

Özdemir, H. (2012). Geomorphometric analysis of Albania river basins. *IBAC*, *2*.

Pashko, P., & Aliaj, S. (2020). Stratigraphy and tectonic evolution of late Miocene-Quaternary Basins in Eastern Albania: A review. *Bulletin of the Geological Society of Greece*, *56*(1), 317–351. https://doi.org/10.12681/bgsg.22064

Pearce, D., Rondenay, S., Sachpazi, M., Charalampakis, M., & Royden, L. H. (2012). Seismic investigation of the transition from Continental to Oceanic subduction along the western Hellenic subduction zone. *Journal of Geophysical Research*, *117*(7). https://doi.org/10.1029/2011JB009023

Phillips, F. M., Argento, D. C., Balco, G., Caffee, M. W., Clem, J., Dunai, T. J., et al. (2016). The CRONUS-Earth project: A synthesis. *Quaternary Geochronology*, *31*, 119–154. https://doi.org/10.1016/j.quageo.2015.09.006

Prince, P. S., Spotila, J. A., & Henika, W. S. (2011). Stream capture as driver of transient landscape evolution in a tectonically quiescent setting. *Geology*, *39*(9), 823–826. https://doi.org/10.1130/G32008.1

Racano, S., van der Beek, P. A., Schildgen, T. F., Faccenna, C., Buleo Tebar, V., & Cosentino, D. (2024). Slab driven Quaternary rock-uplift and topographic evolution in the northern-central Apennines from linear inversion of the drainage system. *Geochemistry, Geophysics, Geosystems*, *25*(7). https://doi.org/10.1029/2024GC011592

Ramsey, L. A., Walker, R. T., & Jackson, J. (2008). Fold evolution and drainage development in the Zagros Mountains of Fars province, SE Iran. *Basin Research*, *20*(1), 23–48. https://doi.org/10.1111/j.1365-2117.2007.00342.x

Reiners, P. W., & Brandon, M. T. (2006). Using thermochronology to understand orogenic erosion. *Annual Review of Earth and Planetary Sciences*, *34*(1), 419–466. https://doi.org/10.1146/annurev.earth.34.031405.125202

Ribolini, A., Bini, M., Isola, I., Spagnolo, M., Zanchetta, G., Pellitero, R., et al. (2018). An oldest Dryas glacier expansion on mount Pelister (former Yugoslavian Republic of Macedonia) according to 10 be cosmogenic dating. https://doi.org/10.6084/m9.figshare.c.3830254

Ribolini, A., Isola, I., Zanchetta, G., Bini, M., & Sulpizio, R. (2011). Glacial features on the Galicica Mountains, Macedonia: Preliminary report. *Geografia Fisica e Dinamica Quaternaria*, *34*(2), 247–255. https://doi.org/10.4461/GFDQ.2011.34.22

Robertson, A., & Shallo, M. (2000). Mesozoic-Tertiary tectonic evolution of Albania in its regional Eastern Mediterranean context. *Tectonophysics*, *316*(3–4), 197–254. https://doi.org/10.1016/s0040-1951(99)00262-0. http://www.elsevier.com/locate/tecto

Rossetti, F., Fellin, M. G., Ballato, P., Faccenna, C., Balestrieri, M. L., Muceku, B., et al. (2024). Building the Albanides by deep underplating. *Tectonics*, *43*(11). https://doi.org/10.1029/2024TC008506

Roucoux, K. H., Tzedakis, P. C., Frogley, M. R., Lawson, I. T., & Preece, R. C. (2008). Vegetation history of the marine isotope stage 7 interglacial complex at Ioannina, NW Greece. *Quaternary Science Reviews*, *27*(13–14), 1378–1395. https://doi.org/10.1016/j.quascirev.2008.04.002

Roure, F., Nazaj, S., Mushka, K., Fili, I., Cadet, J.-P., & Bonneau, M. (2004). Kinematic evolution and petroleum systems—An appraisal of the outer Albanides. In *Thrust tectonics and hydrocarbon systems* (pp. 485–504). American Association of Petroleum Geologists. https://doi.org/10.1306/M82813C25

Roure, F., Scheck-Wenderoth, M., Matenco, L., Muska, K., & Nazai, S. (2013). Dynamics and active processes: The Albanian natural laboratory and analogues. *Italian Journal of Geosciences*, *132*(2), 169–174. https://doi.org/10.3301/IJG.2013.03

Royden, L., & Faccenna, C. (2018). Subduction orogeny and the late Cenozoic evolution of the Mediterranean Arcs. The annual review of Earth and planetary sciences is online at Earth.annualreviews.Org. *Annual Review of Earth and Planetary Sciences*, *46*, 261–289. https://doi.org/10.1146/annurev-earth-060115

Royden, L. H. (1993). Evolution of retreating subduction boundaries formed during continental collision. *Tectonics*, *12*(3), 629–638. https://doi.org/10.1029/92TC02641

Royden, L. H., & Papanikolaou, D. J. (2011). Slab segmentation and late Cenozoic disruption of the Hellenic arc. *Geochemistry, Geophysics, Geosystems*, *12*(3). https://doi.org/10.1029/2010GC003280

Rrezart Bozo, M., Rexhep Kocii, A., Dushi, E., & Begu, E. (2018). Neotectonic features of the albanides orogenic structure. https://doi.org/10.5593/sgem2018/1.1

Sadori, L., Koutsodendris, A., Panagiotopoulos, K., Masi, A., Bertini, A., Combourieu-Nebout, N., et al. (2016). Pollen-based paleoenvironmental and paleoclimatic change at Lake Ohrid (south-eastern Europe) during the past 500 ka. *Biogeosciences*, *13*(5), 1423–1437. https://doi.org/10.5194/bg-13-1423-2016

Schenker, F. L., Fellin, M. G., & Burg, J. P. (2015). Polyphase evolution of Pelagonia (northern Greece) revealed by geological and fission-track data. *Solid Earth*, *6*(1), 285–302. https://doi.org/10.5194/se-6-285-2015

Scherler, D., Bookhagen, B., & Strecker, M. R. (2014). Tectonic control on 10Be-derived erosion rates in the Garhwal Himalaya, India. *Journal of Geophysical Research: Earth Surface*, *119*(2), 83–105. https://doi.org/10.1002/2013JF002955

Schildgen, T. F., Cosentino, D., Bookhagen, B., Niedermann, S., Yildirim, C., Echtler, H., et al. (2012). Multi-phased uplift of the southern margin of the central Anatolian plateau, Turkey: A record of tectonic and upper mantle processes. *Earth and Planetary Science Letters*, *317–318*, 85–95. https://doi.org/10.1016/j.epsl.2011.12.003

Schildgen, T. F., Yildirim, C., Cosentino, D., & Strecker, M. R. (2014). Linking slab break-off, Hellenic trench retreat, and uplift of the central and Eastern Anatolian plateaus. *Earth-Science Reviews*, *128*, 147–168. https://doi.org/10.1016/j.earscirev.2013.11.006

Schumm, S. A. (1993). River response to baselevel change: Implications for sequence stratigraphy. *Source: The Journal of Geology*, *101*(2), 279–294. https://doi.org/10.1086/648221

Schwanghart, W., & Scherler, D. (2014). Short communication: TopoToolbox 2—MATLAB-Based software for topographic analysis and modeling in Earth surface sciences. *Earth Surface Dynamics*, *2*(1), 1–7. https://doi.org/10.5194/esurf-2-1-2014

Serpelloni, E., Cavaliere, A., Martelli, L., Pintori, F., Anderlini, L., Borghi, A., et al. (2022). Surface velocities and strain-rates in the Euro-Mediterranean region from massive GPS data processing. *Frontiers in Earth Science*, *10*. https://doi.org/10.3389/feart.2022.907897

Soto, J. I., Flinch, J. F., & Tari, G. (2017). *Permo-triassic salt provinces of Europe, North Africa and the Atlantic margins: Tectonics and hydrocarbon potential*. Elsevier.

Soto, J. I., Tranos, M. D., Bega, Z., Dooley, T. P., Hernández, P., Hudec, M. R., et al. (2024). Contrasting styles of salt-tectonic processes in the Ionian zone (Greece and Albania): Integrating surface geology, subsurface data, and experimental models. *Tectonics*, *43*(1). https://doi.org/10.1029/2023TC008104

Speranza, F., Islami, I., Kissel, C., & Hyseni, A. (1995). Paleomagnetic evidence for Cenozoic clockwise rotation of the external Albanides. *Earth and Planetary Science Letters*, *129*(1–4), 121–134. https://doi.org/10.1016/0012-821X(94)00231-M

Speranza, F., Kissel, C., Islami, I., Hyseni, A., & Laj, C. (1992). First paleomagnetic evidence for rotation of the Ionian zone of Albania. *Geophysical Research Letters*, *19*(7), 697–700. https://doi.org/10.1029/92GL00575

Stampfli, G. M., & Kozur, H. W. (2006). Europe from the Variscan to the alpine cycles. *Geological Society Memoir*, *32*(1), 57–82. https://doi.org/10.1144/GSL.MEM.2006.032.01.04

Tagari, D., Vergely, P., & Aliaj, S. (1993). Tectonique polyphasee plioquaternaire en Albanie orientale (region de Korca-Progradeci). *Bulletin—Societie Geologique de France*, *164*, 727–737.

Teloni, S., Invernizzi, C., Mazzoli, S., Pierantoni, P. P., & Spina, V. (2020). Seismogenic fault system of the mw 6.4 November 2019 Albania earthquake: New insights into the structural architecture and active tectonic setting of the outer albanides. *Journal of the Geological Society*, *178*(2). https://doi.org/10.1144/jgs2020-193

Twidale, C. R. (2004). River patterns and their meaning. *Earth-Science Reviews*, *67*(3–4), 159–218. https://doi.org/10.1016/j.earscirev.2004.03.001

Ustaszewski, K., Schmid, S. M., Fügenschuh, B., Tischler, M., Kissling, E., & Spakman, W. (2008). A map-view restoration of the alpine-carpathian-dinaridic system for the early Miocene. *Swiss Journal of Geosciences*, *101*(SUPPL.1), 273–294. https://doi.org/10.1007/s00015-008-1288-7

van Hinsbergen, D. J. J., Langereis, C. G., & Meulenkamp, J. E. (2005). Revision of the timing, magnitude and distribution of Neogene rotations in the western Aegean region. *Tectonophysics*, *396*(1–2), 1–34. https://doi.org/10.1016/j.tecto.2004.10.001

van Unen, M., Matenco, L., Nader, F. H., Darnault, R., Mandic, O., & Demir, V. (2019). Kinematics of foreland-vergent crustal accretion: Inferences from the dinarides evolution. *Tectonics*, *38*(1), 49–76. https://doi.org/10.1029/2018TC005066

Velaj, T. (2001). Evaporites in Albania and their impact on the thrusting processes. *Journal of the Balkan Geophysical Society*, *17*(Issue I), 68–78. https://doi.org/10.1007/bf03175658

Vittori, E., Blumetti, A. M., Comerci, V., Di Manna, P., Piccardi, L., Gega, D., & Hoxha, I. (2021). Geological effects and tectonic environment of the 26 November 2019, Mw6.4 Durres earthquake (Albania). *Geophysical Journal International*, *225*(2), 1174–1191. https://doi.org/10.1093/gji/ggaa582

von Blanckenburg, F. (2005). The control mechanisms of erosion and weathering at basin scale from cosmogenic nuclides in river sediment. *Earth and Planetary Science Letters*, *237*(3–4), 462–479. https://doi.org/10.1016/j.epsl.2005.06.030

von Blanckenburg, F., Hewawasam, T., & Kubik, P. W. (2004). Cosmogenic nuclide evidence for low weathering and denudation in the wet, tropical highlands of Sri Lanka. *Journal of Geophysical Research*, *109*(F3). https://doi.org/10.1029/2003jf000049

Wagner, B., Vogel, H., Francke, A., Friedrich, T., Donders, T., Lacey, J. H., et al. (2019). Mediterranean winter rainfall in phase with African monsoons during the past 1.36 million years. *Nature*, *573*(7773), 256–260. https://doi.org/10.1038/s41586-019-1529-0

Whipple, K. X. (2009). The influence of climate on the tectonic evolution of Mountain belts. *Nature Geoscience*, *2*(2), 97–104. https://doi.org/10.1038/ngeo413

Whipple, K. X., & Tucker, G. E. (1999). Dynamics of the stream-power river incision model: Implications for height limits of mountain ranges, landscape response timescales, and research needs. *Journal of Geophysical Research*, *104*(B8), 17661–17674. https://doi.org/10.1029/1999jb900120

Whittaker, A. C. (2012). How do landscapes record tectonics and climate? *Lithosphere*, *4*(2), 160–164. https://doi.org/10.1130/RF.L003.1

Willett, S. D., & Brandon, M. T. (2013). Some analytical methods for converting thermochronometric age to erosion rate. *Geochemistry, Geophysics, Geosystems*, *14*(1), 209–222. https://doi.org/10.1029/2012GC004279

Willett, S. D., Slingerland, R., & Hovius, N. (2001). Uplift, shortening, and steady state topography in active mountain belts. *American Journal of Science*, *301*(4–5), 455–485. https://doi.org/10.2475/ajs.301.4-5.455

Wittmann, H., von Blanckenburg, F., Kruesmann, T., Norton, K. P., & Kubik, P. W. (2007). Relation between rock uplift and denudation from cosmogenic nuclides in river sediment in the central alps of Switzerland. *Journal of Geophysical Research*, *112*(4). https://doi.org/10.1029/2006JF000729

Wobus, C., Whipple, K. X., Kirby, E., Snyder, N., Johnson, J., Spyropolou, K., et al. (2006). Tectonics from topography: Procedures, promise, and pitfalls. *Special Papers - Geological Society of America*, *398*, 55–74. https://doi.org/10.1130/2006.2398(04

Wobus, C. W., Tucker, G. E., & Anderson, R. S. (2010). Does climate change create distinctive patterns of landscape incision? *Journal of Geophysical Research*, *115*(4). https://doi.org/10.1029/2009JF001562

Woodward, J. C., Hamlin, R. H. B., Macklin, M. G., Hughes, P. D., & Lewin, J. (2008). Glacial activity and catchment dynamics in northwest Greece: Long-term river behaviour and the slackwater sediment record for the last glacial to interglacial transition. *Geomorphology*, *101*(1–2), 44–67. https://doi.org/10.1016/j.geomorph.2008.05.018

Woodward, J. C., Hamlin, R. H. B., Macklin, M. G., Karkanas, P., & Kotjabopoulou, E. (2001). Quantitative sourcing of slackwater deposits at Boila rockshelter: A record of lateglacial flooding and Paleolithic settlement in the pindus Mountains, Northwest Greece. *Geoarchaeology—An International Journal*, *16*(5), 501–536. https://doi.org/10.1002/gea.1003

Wortel, M. J. R., & Spackman, W. (2000). Subduction and slab detachment in the Mediterranean-carpathian region. *Science*, *290*(5498), 1910–1917. https://doi.org/10.1126/science.290.5498.1910

Yanites, B. J., Becker, J. K., Madritsch, H., Schnellmann, M., & Ehlers, T. A. (2017). Lithologic effects on landscape response to base level changes: A modeling study in the context of the Eastern Jura Mountains, Switzerland. *Journal of Geophysical Research: Earth Surface*, *122*(11), 2196–2222. https://doi.org/10.1002/2016JF004101

Yanites, B. J., Ehlers, T. A., Becker, J. K., Schnellmann, M., & Heuberger, S. (2013). High magnitude and rapid incision from river capture: Rhine River, Switzerland. *Journal of Geophysical Research: Earth Surface*, *118*(2), 1060–1084. https://doi.org/10.1002/jgrf.20056

Yanites, B. J., Tucker, G. E., & Anderson, R. S. (2009). Numerical and analytical models of cosmogenic radionuclide dynamics in landslide-dominated drainage basins. *Journal of Geophysical Research*, *114*(1). https://doi.org/10.1029/2008JF001088

Zhu, H., Bozdağ, E., Peter, D., & Tromp, J. (2012). Structure of the European upper mantle revealed by adjoint tomography. *Nature Geoscience*, *5*(7), 493–498. https://doi.org/10.1038/ngeo1501

References From the Supporting Information

Balco, G., & Rovey, C. W. (2008). An isochron method for cosmogenic-nuclide dating of buried soils and sediments. *American Journal of Science*, *308*(10), 1083–1114. https://doi.org/10.2475/10.2008.02

Berlin, M. M., & Anderson, R. S. (2009). Steepened channels upstream of knickpoints: Controls on relict landscape response. *Journal of Geophysical Research: Earth Surface Blackwell Publishing Ltd*, *114*(Issue 3). https://doi.org/10.1029/2008JF001148

Flint, J. J. (1974). Stream gradient as a function of order, magnitude, and discharge. *Water Resources Research*, *10*(5), 969–973. https://doi.org/10.1029/WR010i005p00969

Gallen, S. F., Wegmann, K. W., & Bohnenstiehl, D. W. R. (2013). Miocene rejuvenation of topographic relief in the southern appalachians. *Geological Society of America Today*, *23*(2), 4–10. https://doi.org/10.1130/GSATG163A.1

Hack, J. T. (1957b). Studies of longitudinal stream profiles in Virginia and Maryland. *U. S. Geological Survey Professional Paper*, *294-B*, 97.

Haviv, I., Enzel, Y., Whipple, K. X., Zilberman, E., Matmon, A., Stone, J., & Fifield, K. L. (2010). Evolution of vertical knickpoints (waterfalls) with resistant caprock: Insights from numerical modeling. *Journal of Geophysical Research*, *115*(3). https://doi.org/10.1029/2008JF001187

Miller, S. R., Sak, P. B., Kirby, E., & Bierman, P. R. (2013). Neogene rejuvenation of central Appalachian topography: Evidence for differential rock uplift from stream profiles and erosion rates. *Earth and Planetary Science Letters*, *369–370*, 1–12. https://doi.org/10.1016/j.epsl.2013.04.007

Montgomery, D. R., & Gran, K. B. (2001). Downstream variations in the width of bedrock channels. *Water Resources Research*, *37*(6), 1841–1846. https://doi.org/10.1029/2000WR900393

Olivetti, V., Cyr, A. J., Molin, P., Faccenna, C., & Granger, D. E. (2012). Uplift history of the Sila Massif, southern Italy, deciphered from cosmogenic 10Be erosion rates and river longitudinal profile analysis. *Tectonics*, *31*(3). https://doi.org/10.1029/2011TC003037

Perron, J. T., & Royden, L. (2013). An integral approach to bedrock river profile analysis. *Earth Surface Processes and Landforms*, *38*(6), 570–576. https://doi.org/10.1002/esp.3302